TURUN YLIOPISTO

The role of gut microbiota in meeting different host energy requirements early in life

Master of Science / Department of Biology

Master's thesis

Helka Vento

18.5.2026

Turku

Programme, subject: Master of Science, Biology, Physiology and Genetics

Author: Helka Vento

Title: The role of gut microbiota in meeting different host energy requirements early in life

Supervisors: Anni Hämäläinen, Santosh Lamichhane

Number of pages: 55

Date: 18.5.2026

Animals can cope with fluctuating food availability via phenotypic plasticity. Food restriction may have particularly strong or lasting phenotypic effects when encountered in early life (via maternal undernutrition) or by individuals with high intrinsic energy needs (fast metabolism).The gut microbiota can potentially mediate reversible plasticity by interacting with host metabolism, e.g., via short-chained fatty acids (SCFAs). I examined the gut microbiota's role in shaping early-life nutrition-dependent plasticity in individuals with inherently different energy requirements by analysing data from a diet manipulation experiment in experimentally evolved fast-metabolism (A) and control (C) lines of the bank vole (*Myodes glareolus*). Dams were fed standard diet (SD) or restricted diet (CR) during gestation and lactation. Weaned offspring were fed SD for a recovery period to study lasting phenotypic effects. Litter size, growth, gut microbiota, and cecal SCFA concentrations of the offspring were examined. The response to maternal CR was mostly reversible and similar in both selection directions: the A-lines were bigger at birth and weaning, with a temporary CR-induced decrease at weaning in both selection directions. Beta (but not alpha) diversity metrics suggested a weak, persistent, selection-dependent response to CR. However, differentially abundant genera were only identified in response to CR. Out of the quantified SCFAs, only butyrate was elevated after recovery in both selection directions. These results suggest that the A-lines can adapt to maternal CR with similar success as the C-lines, with partial evidence for lasting impact on microbial metabolism and a distinct response in microbiota community, which may signal microbiota-modulated adaptation.

Key words: gut microbiota, phenotypic plasticity, metabolic rate, short-chained fatty acids, experimental evolution

Koulutusohjelma, oppiaine: Filosofian maisteri, Biologia, Fysiologia ja genetiikka

Tekijä: Helka Vento

Otsikko: The role of gut microbiota in meeting different host energy requirements early in life

Ohjaajat: Anni Hämäläinen, Santosh Lamichhane

Sivumäärä: 55

Päivämäärä: 18.5.2026

Eläimet voivat selviytyä vaihtelevista ravinto-olosuhteita fenotyyppisen plastisuuden avulla. Ravinnon niukkuudella saattaa olla pysyvämpiä tai voimakkaampia vaikutuksia varhaiselämässä (äidin aliravitsemuksen välityksellä) tai yksilöillä, joilla on synnynnäisesti korkeammat energiatarpeet (nopea aineenvaihdunta). Suolistomikrobisto saattaa toimia palautuvan fenotyyppisen plastisuuden välittäjänä osallistumalla isännän energiametaboliaan esim. lyhytketjuisten rasvahappojen (SCFA) välityksellä. Tässä tutkielmassa tarkastelen suolistomikrobiston osuutta varhaiskehityksen ravitsemusperäisen plastisuuden säätelijänä yksilöillä, joilla on synnynnäisesti erilaiset energiatarpeet. Analysoin aineistoa ravintomanipulaatiokokeesta metsämyyrän (*Myodes glareolus*) korkean aineenvaihdunnan kokeellisilla valintalinjoilla (A) sekä niiden kontrollilinjoilla (C). Tiineys- ja imetysaikana emoille syötettiin joko vakioruokaa (SD) tai kalorirajoitettua ruokaa (CR). Vieroitusiän jälkeen kaikki poikaset saivat vakioruokaa palautumisjakson ajan, ja poikuekokoa, poikasten kasvua, suolistomikrobistoa, sekä umpisuolen (*cecum*) SCFA-konsentraatiota tarkasteltiin. Vaste CR-käsittelyyn oli pääsääntöisesti palautuva ja samansuuruinen kummassakin selektiosuunnassa. A-linjan jälkeläiset olivat suurikokoisempia syntymässä sekä vieroitusiässä. CR-käsittelyssä vieroitusikäiset poikaset olivat pienempiä kummassakin selektiosuunnassa. Betadiversiteetissä (muttei alfadiversiteetissä) havaittiin viitteitä CR-käsittelyn lievästä, selektioriippuvaisesta vaikutuksesta suolistomikrobistoon. Merkitsevästi runsaussuhteissaan muuttuneita bakteerisukuja havaittiin kuitenkin vain vasteena CR-käsittelyyn. Kvantifioiduista SCFA:ista vain butyraatti oli koholla palautumisjakson lopussa kummassakin selektiosuunnassa. Tulokset viittaavat siihen, että A-linjat pystyvät sopeutumaan kehitysaikaiseen kalorirajoitteeseen yhtä hyvin kuin C-linjat, ja osittaisia viitteitä havaittiin pysyvistä muutoksista suolistomikrobiston metaboliittituotannossa CR-käsittelyssä sekä selektioriippuvaisesta suolistobakteeriyhteisön vasteesta CR-käsittelyyn, mikä saattaa viitata suolistomikrobiston moduloimaan adaptaatioon.

Avainsanat: suolistomikrobisto, fenotyyppinen plastisuus, perusaineenvaihdunta, lyhytketjuiset rasvahapot, kokeellinen evoluutio

Table of contents

1 Introduction

Food quality and quantity typically fluctuate during an individual's lifetime, requiring organisms to cope with phenotypic plasticity (i.e. changes in physiology, morphology or behavior not associated with genetic changes). The capacity for phenotypic plasticity, constrained by the individual's genotype, emerges as an important contributor to fitness. Individual heterogeneity represents the population's adaptive potential to various environments. However, the challenge posed by nutritional limitations (and the warranted phenotypic response) may vary between individuals with different basal metabolic rates and energy expenditure (Glazier and Gjoni 2024). Phenotypic plasticity can be reversible, meaning that the phenotype reverts after the environmental driver subsides, or irreversible, in which case the environmental conditions at a sensitive time-window shape the individual's phenotype indefinitely. Environmental stress early in life can bring about persistent phenotypic changes that are initially adaptive but may later turn pathological if environmental conditions change. Early-life nutritional stress is extensively studied due to its relevance in human health (Barker et al. 1993). Maternal undernutrition during gestation is a prime example of environmental cues irreversibly shaping the offspring's phenotype: it "programs" the offspring to an altered metabolic state, the "thrifty phenotype", which promotes early life survival through efficient energy utilization, but later subjects the individual to symptoms of metabolic syndrome, such as obesity and propensity to develop type 2 diabetes (Hales and Barker 2001).

In addition to genotype-environment interactions in shaping plasticity, the mammalian symbiotic gut microbiota has emerged as a potential mediator of phenotypic plasticity through its influence on host energy metabolism. Bacteria are not bound by the relatively long generation times of mammals, which allows the community to respond swiftly to new environmental pressures (i.e. the quality and quantity of food that the host consumes) with a shift in community composition and metabolic output (Amato 2013). Bacteria contribute to the host energy metabolism by fermenting insoluble fiber into short-chained fatty acids (SCFAs), that are utilized for energy in the gut and distal tissues, contributing up to 70 % of daily dietary energy depending on the species (Amato 2013; Bergman 1990; den Besten et al. 2013). Environmentally induced changes in the

community composition or biochemical activity of symbiotic bacteria can help the host cope with starvation by improving energy intake efficiency (Mestdagh et al. 2012), e.g., via a shift in the amount or type of SCFA produced (Morrison and Preston 2016),

Although individual heterogeneity in gene-environment interactions, early-life determinants of irreversible plasticity, and the gut microbiota are all subjects of considerable interest in diverse fields ranging from evolutionary biology to medicine, their interplay is yet incompletely understood. In this thesis, I examine the persistence of the effects of maternal nutritional stress during gestation and lactation on the offspring and their symbiotic microbiota in experimental selection lines of the bank vole (*Myodes glareolus*) with different energy requirements. Sadowska et al. (2008) originally established these selection lines from bank voles captured from the field to address the ongoing debate on the evolution of basal metabolic rate (BMR) in terrestrial vertebrates, particularly to test the hypothesis that high BMR emerged as a by-product of selection for high locomotor activity. A-line voles were selected for high voluntary oxygen consumption during a swimming trial (VO_2 swim), whereas C-lines were maintained without directional selection. In addition to VO_2 swim, the A-lines evolved a higher BMR, which suggests higher maintenance energy requirements (Sadowska et al. 2015). Accordingly, the A-lines also consume more food in comparison to the C-lines (Dheyongera et al. 2016). This makes them a suitable model to represent heritable differences in metabolic rate and energy expenditure.

1.1 Metabolic rate and life history tradeoffs

Life history strategy describes how animals allocate energy to fitness-essential functions such as survival, growth, and reproduction. BMR represents the energetic cost of living and is thus a key component in an organism's energy allocation scheme. The "pace of life" that varies on the fast-slow axis is set by the organism's metabolic rate together with life history strategies, which are evolutionary coupled (Auer et al., 2018). Fast-paced individuals invest in early growth and reproduction, while their slow-paced counterparts grow and reproduce slower, but also live a longer time. Factors behind individual heterogeneity in metabolic rate are complex and numerous, and include body mass and organ size, maternal and developmental effects, and

environmental cues (Burton et al., 2011). The relationship of metabolic rate and fitness has been studied extensively, with mixed evidence across different animals and fitness-related traits (Arnold et al., 2021). According to the "context-dependent" hypothesis, metabolic rate is associated with fitness, but this relationship depends on the prevailing environmental context, e.g. food availability (Burton et al., 2011). The meta-analysis by Arnold et al. (2021), found a positive correlation between various fitness-related traits and resting metabolic rate, but no significant associations with measures of absolute fitness (i.e. reproduction and survival). They note that most laboratory studies included in the analysis provide high-quality food *ad libitum*, which does not correspond to the spatially and temporally fluctuating resource availability in nature. The relationship between metabolic rate, life history traits and fitness in relation to the environment is thus still incompletely understood.

In addition to intrinsic factors, the metabolic phenotype is further modulated by the environment. In juvenile trout, standard metabolic rate (SMR) is modulated based on food availability in a way that maximizes the growth under the prevailing conditions, with no association between the baseline SMR and the capacity for change (Auer et al., 2015). Furthermore, the gut microbiota contributes to the host's energy metabolism, e.g. by metabolizing compounds that the host lacks the enzymatic means to break down. Turnbaugh et al. (2006) demonstrated a causal link between gut microbiota and metabolic phenotype by transplanting microbiota from obese and lean mice to gnotobiotic recipient mice. In the mice that received the transplantation from obese mice energy harvest and fat storage were increased compared to the mice that received the transplantation from lean mice. Additionally, Walters et al. (2020) linked geographic variation in *Drosophila* life history traits to differences in microbiota composition, and found that both local adaptation and microbiota shape the life history genotype: locally adapted isogenic fly lines reared with different microbiota allocate resources differently into reproduction and somatic maintenance. In wild flies the abundance of these bacteria co-varies with life history strategy, and in bacteria-free flies inoculation with the relevant bacteria can suppress or reverse the life history differences.

1.2 Gut microbiota as a mediator of phenotypic plasticity

The omnipresence of symbiotic microbes across the plant and animal kingdoms, together with growing understanding of complex interactions and dynamics between the host and its associated microbiota, has led to the emergence of the holobiont concept. This framework reconceptualizes the host and its microbiota as a distinct biological unit (Bordenstein & Theis, 2015; Rosenberg & Zilber-Rosenberg, 2018). In mammals, the initial colonizing taxa are inherited from the mother via inoculation in the birth canal and in milk during nursing (Martínez-Oca et al., 2023; Stewart et al., 2018). Commensal microbes can also be acquired horizontally from the environment, which creates additional potential for diversity and flexibility during the host's lifetime (Amato, 2013). This is leveraged in therapeutic fecal transplants, where modifications to the patient's gut microbiota are used to bring a dysbiotic microbial community to a state protective of disease. Furthermore, bacteria may adapt and maintain flexibility by horizontal gene transfer, novel mutations, or epigenetic regulation of bacterial or host genes (Dapa et al., 2023; Voolstra & Ziegler, 2020).

Although the initial microbes colonizing the gut come from the mother, the diet is the strongest determinant of gut microbiota composition (Amato, 2013; David et al., 2014), with a significant change observable within days of dietary alteration (Turnbaugh et al., 2006). The host directly modifies the environment experienced by the gut microbiota by the quality and quantity of ingested food. As food availability fluctuates, various selective pressures are imposed on the microbial community, driving a change in the gut microbial community. This ability to rapidly and dynamically respond to dietary change has provoked interest in the gut microbiota's capacity to mediate reversible phenotypic plasticity by buffering against changing nutritional conditions (Amato, 2013). To reversibly and dynamically adapt to fluctuating changes in diet, the gut microbiota must retain core functionality under changing selection pressures. Diet-induced changes in the microbiota composition are typically reversible and initial diversity, evenness and functional redundancy promote recovery speed and resilience (Bourdeau-Julien et al., 2023; Voolstra & Ziegler, 2020). Indeed, functional redundancy is characteristic to microbiota communities; individuals may vary in the taxonomic composition of their microbiota but not its functional capacity (Doolittle & Booth, 2017).

Diet-induced changes in the microbiota influence bacterial production of SCFAs, which power the cells of the intestinal barrier and participate to various metabolic processes in distal organs (den Besten et al., 2013), acting as a bridge between microbiota and host metabolism.

1.3 Short-chained fatty acids

The microbiota can extract nutrients from food that the hosts lack the enzymatic means to break down. A particularly important group of metabolites produced by the microbiota are short-chained fatty acids (SCFA) that bacteria ferment from non-digestible carbohydrates (dietary fiber), which make up 10-70% of daily calorie requirements depending on the species (Bergman, 1990). In addition to being used for energy, SCFAs participate in fatty acid, glucose, amino acid, and cholesterol metabolism (den Besten et al., 2013). The three major SCFAs produced by the microbiota are acetate, propionate and butyrate, which are differentially utilized in host tissues (den Besten et al., 2013). Out of the three major SCFAs produced by the gut microbiota, acetate is by far the most prevalent, contributing about 60 % of the total SCFAs, while propionate and butyrate contribute 20 % each (Fusco et al., 2023). In rodents, the fermentation of dietary fiber into SCFAs primarily takes place in the cecum, and requires co-operation of the fermenters with the host and the surrounding microbial community: the fermentation process modifies the pH of the intestinal lumen, which limits the fermentation process and requires stabilization by other gut bacteria and the host (den Besten et al., 2013).

Up to 95 % of SCFAs are swiftly absorbed by colonocytes (i.e. epithelial cells lining the colon) and utilized there for energy (den Besten et al., 2013). Colonocytes have the highest affinity for butyrate, making it their preferred energy source. However, the contribution of acetate is likely equally important because of its higher concentration (den Besten et al., 2013). SCFAs, particularly butyrate, are important for the integrity of the intestinal lining: In germ free mice that lack microbiota-derived SCFAs, colonocytes undergo autophagy, which can be prevented by supplying the mice with butyrate-producing gut bacteria or treating isolated colonocytes with butyrate (Donohoe et al., 2011). The majority of acetate that enters the circulation is metabolized in the liver,

where it is used as an energy source and a substrate for cholesterol, fatty acid, and amino acid synthesis, with the rest utilized in other tissues such as the heart, kidney and muscle (den Besten et al., 2013). Circulating propionate is used as a gluconeogenesis precursor in the liver (den Besten et al., 2013).

Importantly, bacterial taxa differ in the type of SCFAs they metabolize from food. Firmicutes, for example, are major butyrate producers, while Bacteroidetes generally specialize in propionate and acetate production (den Besten et al., 2013). By shifting the SCFA production in quality and/or quantity, the microbiota can modulate energy utilization capacity and allocation among tissues in response to changes in diet (Morrison & Preston, 2016), by for example, increasing the proportion of butyrate-producing Firmicutes. SCFA production also depends on the amount and type of available dietary fiber in the host's diet (den Besten et al., 2013): β-glucans and pectin, for example, are highly fermentable while cellulose is poorly fermented in non-ruminants (Holscher, 2017). Although cellulose does not increase total SCFA concentration, it induces changes in the gut microbiota's community composition in mice (Wen et al., 2022).

1.4 Early-life nutrition and irreversible plasticity

In mammals, irreversible phenotypic plasticity is primarily determined during ontogeny through the mother's physiology. Pre-natal malnutrition can shape the offspring's phenotype irreversibly and influence long-term health outcomes: In humans and rodents, gestational energy deficiency "programs" the individual to an altered metabolic state, the "thrifty phenotype", which promotes early life survival through efficient energy utilization, but later subjects the individual to symptoms of metabolic syndrome, including obesity, hypertension, glucose intolerance, and elevated insulin and triglycerides, increasing the risk of adverse health outcomes under conditions of high energy availability (Barker et al. 1993; Desai and Hales 1997; Hales and Barker 2001). However, moderate calorie restriction during lactation can have a prolonged protective effect against obesity in rats (Palou et al. 2010), indicating that the timing and severity of early life calorie restriction matters for the long-term outcome.

Even under benevolent nutritional conditions, the maternal microbiota goes through changes during the pregnancy, with certain taxa becoming more abundant to support nutrient supply for fetal development (Koren et al. 2012). The gut, vaginal, and placental microbiota of overweight mothers differ in their composition from those of healthy-weight mothers (Strobel, Juul, and Hendrixson 2023). The environment also shapes the maternal microbiota: Dietary intake including fat, fruit and vegetable, and animal protein sources during gestation are associated with certain shifts in gut, vaginal and milk microbiome composition, which in turn influence the offspring microbiome (Strobel et al. 2023). Maternal stress can change the composition of vaginal microbiome subsequently altering the initial colonizing community the offspring receives during birth (Jašarević et al. 2015). In mice, maternal calorie restriction impacts the milk microbiota during lactation, which influences the bacterial colonization process of the gut in the offspring and can be associated with adverse health outcomes (Martínez-Oca et al., 2023).

1.5 Aims and hypotheses

Given the long-term effects of early-life nutritional conditions on host physiology and the growing recognition of the microbiota as a contributor to host metabolism, this thesis aims to examine the effects of maternal undernutrition in offspring and gut microbiota composition. In particular, our objective was to study whether these responses differ between experimentally selected bank vole lines with contrasting energy requirement, serving as a model for intrinsic differences in metabolic rate.

The central hypothesis is that A-lines, characterized by high metabolic rate and greater energy requirements, will suffer more from maternal calorie restriction in terms of reproductive success and offspring growth. However, these effects may be alleviated by a greater compensatory shift in microbial community composition and/or their metabolic output. Because the calorie restriction is experienced at a sensitive developmental window, the associated changes may persist even after conditions return to normal.

To test these hypotheses, this thesis leverages existing data from a diet manipulation experiment conducted in 2020 as a collaboration between the Jagiellonian University

and the University of Jyväskylä. Females from A (high metabolism) and C (control) selection lines were fed either a standard diet (SD) or a diet diluted with 30% cellulose (CR30) from mating until weaning, covering the entire developmental period during which offspring depend on maternal nutrition. After weaning, all offspring fed the standard diet for a recovery period to assess whether the effects of maternal undernutrition persist after nutritional conditions normalize.

2 Materials and methods

2.1 Model species

The voles used in this study are from a long-term selection experiment on bank voles selected either for maximum voluntary oxygen consumption in a swimming trial (A) or maintained without selection (C) with four parallel lines of each selection direction (Sadowska et al., 2008). As reported by Sadowska et al. (2005, 2008), the initial laboratory population was reared in 2000-2001 from 320 voles captured from Niepolomice Forest in southern Poland. The base population for the selection experiment consisted of roughly 1,000 individuals from 159 pairs, which were assigned randomly to one of the four parallel lines of each selection direction (including 8 lines of herbivorous and predatory selection direction that are not included in this thesis), whose offspring formed the generation 0 of the selection experiment. After 22 generations of selection, the A-lines have evolved 60% higher swim-induced metabolism and significantly higher resting metabolic rate compared to the C lines (Jaromin et al., 2019). In previous studies, only minor differences between the microbiota communities of A-lines and C-lines have been observed in laboratory conditions, but differences microbiota diversity, community composition, and resilience emerge when the bank voles are subjected to field conditions (Hanhimäki et al., 2022). The voles entering the experiment had undergone 30 generations of selection.

2.2 Ethical statement

The research protocols were reviewed and approved by the bioethical committee of the Second Local Institutional Animal Care and Use Committee in Kraków, Poland.

2.3 Animal husbandry

Prior to enrollment in the experiment, animals were maintained under standard conditions in animal facilities at the Jagiellonian University. Non-breeding voles were housed in single-sex groups of about three individuals from the same line type. The cages were equipped with bedding and an upturned coconut shell for enrichment and

shelter. Food (standard rodent chow: energy 12.7 MJ/kg, 24 % protein, 3 % fat, 4 % fiber; Labofeed H, Kcynia, Poland) and water were available ad libitum.

The same rodent chow as in maintenance was used in the breeding colony as the standard diet, and the cellulose-diluted diet was produced by the manufacturer by adding 15% (CR15) or 30% (CR30) cellulose before pressing the chow into pellets. The metabolizable energy content of the diets in kJ/g dry mass was 14.37 for SD, 12.12 for CR15, and 9.86 for CR30. Animals from both selection directions were maintained in the same rooms and were thus exposed to shared environmental bacteria under standard conditions. The measurements and samples described here are a subset of the data collected during the experiment; additional data that are not in the scope of this thesis and thus excluded from this report included measurements of resting metabolic rate, thermogenic capacity, home cage activity, body fat content and organ masses.

2.4 The diet manipulation experiment and sample processing

Females from the breeding colony were selected for the experiment when they had successfully delivered two litters and were gravid with their third litter. Gravid females were observed daily and mated immediately after delivery during post-partum estrus. The third litter and the male were removed a day later, and the females (presumably pregnant with their fourth litter), were housed individually and placed on one of the experimental diets: standard diet (SD) or calorie-restricted diet (CR). Food was available *ad libitum*. Average daily food consumption was recorded based on the difference in the dry weight of previously provided food and food left in the feeder by next feeding. The females assigned to CR diet were fed food diluted with 15% cellulose (CR15) for the first 6 days as an adjustment period. After this they were given food diluted with 30% cellulose (CR30) until the focal fourth litter was weaned.

Females that did not show signs of pregnancy by day 25 were removed from the experiment. A total of 111 litters were enrolled in the experiment (59 C, 52 A). One day after the focal fourth litter was born, the number of live and dead pups was recorded. Live pups were marked permanently by toe clipping, weighed to the nearest 0.001 g, and their sex was determined based on anogenital distance. Sex was determined again at weaning, to correct any misassigned pups. The pups were monitored regularly during

nursing, recording their individual growth and the size of the litter. The pups were counted and weighed on days 1, 5, 9, 13, and 17 after birth. Head width (structural size) was measured at weaning (day 17 after birth).

The pups were weaned on the 17th day after birth following the breeding colony standard protocol. A fecal sample was collected from the dam by placing the animal in an empty cage without bedding or food for 45 minutes, during which water was provided *ad libitum*. The samples were immediately cooled and stored at -80℃ until DNA extraction. Extracts were stored at -80℃ until sequencing. Within a day of weaning the dam was anesthetized and euthanized with isoflurane inhalation overdose and immediately dissected to collect a cecum sample by dissecting out the cecum and gently squeezing as much of the content as possible into a cryovial using sterile tools. Up to 2 female and 2 male pups from each litter were randomly selected with a raffle system for the recovery phase of the experiment, resulting in a total of 306 pups. Remaining 83 pups were euthanized and dissected on the following days (age 18 days) to collect cecum samples.

During the recovery phase (days 17-33) all 306 pups, regardless of maternal diet, were fed a standard diet. According to the breeding colony standard protocol, littermates were housed together up until day 25, then housed individually. Their growth and survival were monitored periodically on days 21, 25, 31, and 33. On day 33 the fecal samples were collected, and the pups were dissected immediately to collect cecum samples as above.

Food consumption was monitored by weighing added food at the beginning of a feeding interval and the food left in the feeder by the end of feeding interval. The dry weight of leftover food was determined by drying the food in an oven before weighing. New food's moisture percentage was measured by comparing the ratio of wet and dry mass in a sample from the food.

2.4.1 Amplicon sequencing

DNA was extracted from the samples using DNeasy Power Soil Pro kit (Qiagen, Germany) following manufacturer instructions. The samples were amplified for the 16S

rRNA V3-V4 segment in PCR 341f-806r primer sequences (CCTAYGGGRBGCASCAG-GGACTACNNGGGTATCTAAT) and sequenced on Illumina MiSeq paired-end sequencing at Novogene (United Kingdom). A total of 704 samples (excluding negative controls) were sequenced, consisting of 174 samples from the dam, 83 from weaning-aged pups and 447 from post-recovery pups. Paired-end reads were demultiplexed, quality filtered according to *fastp* software to remove sequences with low quality, high error rate and excessive ambiguous bases, and filtered to remove chimeras at the sequencing facility (Novogene, United Kingdom) prior to data delivery.

2.4.2 SCFA quantification

Cecal samples collected at dissection from weaning and post-recovery pups were snap frozen in liquid nitrogen immediately after euthanasia, stored at -80℃ and delivered on dry ice to be analyzed at Turku Bioscience Center. The SCFA (acetic, butyric, propionic, hexanoic, octanoic, isovaleric, isobutyric, and valeric acid) quantification was conducted using UHPLC-qToF-MS after applying the 3-nitrophenylhydrazin (3-NPH) derivatization method, as previously described and adapted from liquid chromatography-mass spectrometry (LC-MS) + derivatization method (Lamichhane et al., 2026). A total of 243 samples were analysed, consisting of 18 samples from weaning-aged pups and 225 samples from post-recovery pups. 13 samples were re-analysed due to technical errors, and the values from the later analysis were used in subsequent analyses. The data were preprocessed and normalized to ng/mg in dry weight prior to delivery, which I used in downstream analyses.

2.5 Data analysis

2.5.1 The effects of maternal calorie restriction on reproduction and growth

R 4.5.0 (R Core Team, 2025) was used for data analysis and R packages *ggplot2* (version 4.0.2) (Wickham, 2016) and *cowplot* (version 1.2.0) (Wilke, 2025) for visualizations.

To assess maternal investment in the pups, I fit a generalized linear mixed model with a Conway-Maxwell Poisson distribution to litter size at day 1 and day 17 using the package *glmmTMB* (version 1.1.14) (McGillycuddy et al., 2025). The fixed effects were interaction

and main effects of treatment (SD vs. CR diet) and selection direction (C, A), with parallel line (C1-4, A1-4) as random intercept.

To examine the effects on pup growth in different selection directions, I fit linear mixed models (with Satterthwaite's method for estimating degrees of freedom) to pup body mass (BM) at birth, weaning and after recovery and head width (HW) at weaning using the R package *lme4* (version 2.0.1) (Bates et al., 2015) and *lmerTest* (version 3.2.1) (Kuznetsova et al., 2017). Sex (F, M) and the interaction and main effects of maternal diet and selection direction were fixed effects in all models. The main effect of litter size was included in body mass and head width models at birth and weaning when the pups were still dependent on shared resources from the mother, because the mother's resource investment per pup is smaller in larger litters (T. A. Oksanen et al., 2001). Litter ID nested in parallel line was included as a random intercept in all models to account for pseudoreplication. The significance of the interaction was tested by comparing nested models with ANOVA and dropped from the final model unless significant.

To assess whether the individuals compensate for decreased energy density in the food by eating more, I calculated the average daily food consumption of dams and pups based on the difference in previously added food and food left in the feeder at the end of the feeding interval (3-4 days). The wet and dry weight of feed were measured periodically, and I used the average moisture percentage (4% and 3% in dams and pups, respectively) to estimate the dry weight of added food. In dams, average food consumption was calculated over the days 9-13 after the litter was born. This period was chosen because closer to weaning (day 17) the pups may gradually start eating solid food alongside the mother, which would inflate the dam's food consumption estimate. In pups, food consumption was calculated over the days 21-31 after birth. I fit linear mixed models (with Satterthwaite's method for estimating degrees of freedom) to average daily food consumption in dams and pups, respectively, using the package *lme4* (version 2.0.1) (Bates et al., 2015) with *lmerTest* (version 3.2.1) (Kuznetsova et al., 2017). The interaction and main effects of treatment and selection were included as fixed effects in both models. The model for dams' food consumption also contained fixed effect of litter size (at weaning) and the random intercept of parallel line, whereas the model for pups' food consumption contained the fixed effect of sex and the random

intercept of litter ID nested in parallel line. The significance of the interaction was tested by comparing nested models with ANOVA and dropped from the final model unless significant. Informed by model results, I calculated the estimated marginal means with Kenward-Rogers degrees of freedom for the combinations of treatment and selection for the full model (including the interaction term) using the package *emmeans* (version 2.0.3) (Lenth & Piaskowski, 2017). The proportional change in daily soluble energy intake in each selection direction on different diets was calculated based on the estimated marginal means and the feed energy content (SD 12.7 MJ/kg, CR30 8.9 MJ/kg).

2.5.2 Sequencing data processing

Amplicon sequencing data was processed using Puhti high-performance computing system (CSC Finland). Due to technical/human error, some amplicon sequencing data were lost, leaving data from only 665 preprocessed samples for downstream analyses. I summarized the available data using *FastQC* (version 0.12.1) (Andrews, 2010) and *MultiQC* (version 1.3.) (Ewels et al., 2016). There was a total of 57,078,051 reads across the 665 samples with a per-sample median of 87,036.0 and mean of 85,831.66 (minimum 8,943, maximum 125,01) reads.

The following analyses were done using *Qiime2-amplicon* (version 2025.4) (Bolyen et al., 2019; McDonald et al., 2012; McKinney, 2010). I further quality filtered the effective reads using *quality-filter q-score* method (Bokulich et al., 2013) with a window size of three and threshold of 30 PHRED. This method tolerates three consecutive bases below the threshold quality before the read is truncated at the beginning of the window. I used the default minimum length fraction of 0.7, stating that reads truncated to less than 70% of their original length should be discarded. Zero ambiguous bases were tolerated. 49,087,696 reads passed the quality filters (with 7,990,355 discarded). The reads were then dereplicated and denoised using *Deblur* (Amir et al., 2017), with trim length set to 400 and the minimum number of reads at 10. The trim length of 400 was chosen based on the *MultiQC* report, which showed two major peaks at 400 bp and 420 bp.

To assign taxonomy to the amplicon sequence variants (ASVs), I trained a naïve bayes classifier using *Qiime2 RESCRIPt* (Robeson et al., 2021), according to the tutorial (*Processing, Filtering, and Evaluating the SILVA Database (and Other Reference*

Sequence Data) with RESCRIPt - Community Contributions / Tutorials, 2020). The classifier was trained using SILVA 138.2 SSU Ref NR 99 database (Chuvochina et al., 2026) with species labels included. Database sequences with more than 5 ambiguous bases or homopolymers longer than 8 bases were removed. The remaining sequences were filtered based on taxonomy, removing sequences matching the following criteria: Archaeal 16S longer or equal to 900 bp, bacterial 16S longer or equal to 1,200 bp or eukaryote 18S longer or equal to 1,400 bp. Remaining sequences were dereplicated by removing sequences that were identical in both sequence and taxonomy but identical sequences with different taxonomy were retained. The database sequenced were trimmed to the focal V3-V4 region using the 341f-806r primer sequences (CCTAYGGGRBGCASCAG-GGACTACNNGGGTATCTAAT) that were previously used to amplify the amplicon in the samples. The dereplication step was then repeated to remove redundancy introduced by shortening the region. The classifier was fit with *Qiime2 RESCRIPt* method *evaluate-fit-classifier* (Bokulich et al., 2018), which also performs an evaluation by presenting the full training data to the classifier. This gives the best theoretical classification performance. The F-scores in this evaluation were > 0.98 down to family-level with a drop to 0.946 on genus level and 0.641 on species level. I also performed a 5-fold cross-validation using *RESCRIPt cross-validate* method to assess how well the classifier generalizes to unseen data. The F-scores in this evaluation were > 0.96 down to family level, 0.895 on genus level, with a considerable drop to 0.386 on species level. In summary, the classifier was expected to perform well down to genus level, but not on species-level.

I applied the classifier to assign taxonomy to the ASVs found in the samples with the *Qiime2* method *feature-classifier classify-sklearn* (Bokulich et al., 2018; Pedregosa et al., 2011), with a confidence threshold of 0.7 to limit the taxonomic depth of classification. I then filtered the sequences based on taxonomy, excluding features classified as mitochondrial, chloroplast or archaeal. 10,179 features passed the filters. Feature frequency per sample was 2,833-69,007 with a median of 29,613 median and mean of 30,667. Frequency per feature varied between 10 (as less abundant features were excluded) and 1,754,711 with a median of 31 and mean of 2,004. The total frequency of features in all 665 samples was 20,393,237. Finally, a phylogenetic tree

was constructed using *Qiime2 phylogeny align-to-tree-mafft-fasttree* method with default settings.

Kit-specific contaminant sequences in the samples were examined with negative controls, i.e. empty kits processed in the same way as real samples at regular intervals during the extraction process. In the negative samples, DNA concentration was predominantly low (min = -0.155 ng/µl, median = 1.340 ng/µl, max = 218.925 ng/µl), but forced sequencing produced a median of 21,069 (ranging from 8,943 to 100,067) reads per negative control. Possible contaminants were identified using R package *decontam* (version1.30.0) (Davis et al., 2017), using the prevalence method with the threshold of 0.5, which flags ASVs that are more prevalent in negative controls than in true positive samples as contaminants. This, however, resulted in 1,408 putative contaminants (results not shown), including common bank vole gut bacteria, which suggests contamination between the negative controls and samples rather during extraction or sequencing runs than contaminants originating from kit chemicals. If kit reagents were contaminated, increasing or stable DNA concentration and ASV count would be expected in extraction controls over the usage time of each kit/reagent batch. No such association was found, so the contamination is expected to be random. Because of vole bacteria contamination, the extraction controls could not be used to reliably identify kit contaminants, which is why all features were retained for downstream analyses.

2.5.3 Bacterial diversity and community composition

I converted the *Qiime2* output (rooted phylogenetic tree, ASV table, taxonomy) into a *phyloseq* (version 1.54.2) (McMurdie & Holmes, 2013) object for downstream analyses using the package *qiime2R* (version 0.99.6) (Bisanz, 2018). *Clostridium innocuum* has previously been found to alter microbiota diversity in the experimental vole lines (Lipowska et al., 2025). Contrary to previous work in the colony, where the proportion of hosts carrying this bacterium was low, I observed C. innocuum in 55% of the samples. Therefore, instead of removing these samples from the analyses as in (Lipowska et al. 2025), I flagged their presence for each sample so it can be considered in modeling. The samples were rarefied to even depth of 9,700 using R package *phyloseq* (version 1.54.2) (McMurdie & Holmes, 2013) which resulted in exclusion of 4 (non-negative control)

samples. Rarefaction as a normalization method for next generation sequencing data has been controversial (McMurdie & Holmes, 2014), but according to Schloss (2024), it is currently the best method for microbiota data normalization.

I calculated the alpha diversity metrics of observed ASV count and Shannon index in each rarefied sample using *phyloseq* (version 1.54.2) (McMurdie & Holmes, 2013). ASV count is the raw number of taxa present and Shannon index accounts for both species richness and the relative abundance of taxa (evenness). I analyzed the fecal and cecal samples in weaning-aged and post-recovery pups separately (post-recovery cecum n = 141, post-recovery feces n = 259, weaning cecum n = 82) to assess the acute and long-term effects of maternal calorie restriction on the offspring. I fit generalized linear mixed models with the negative binomial distribution (nbinom1, log-link) to ASV count in the different group/sample type combinations using the R package *glmmTMB* (version 1.1.14) (McGillycuddy et al., 2025). The fixed effects were sex, *C. innocuum* presence, and the interaction and main effects of maternal diet and selection direction, with litter ID nested in parallel line as random intercept. When the models were singular due to zero variance in one level of the nested random effect, the random intercept structure was simplified to contain only the level with non-zero variance. The interaction term was tested for significance with type III marginal F test using *emmeans* (version 2.0.3) joint tests (Lenth & Piaskowski, 2017) and dropped from the final model if statistically non-significant to examine the main effects. In the model for ASV count in weaning group's cecal samples, the random intercept of litter ID nested in parallel line resulted in singularity and convergence failure, so a simplified random intercept of litter ID was used instead. Marginal and conditional R^2 values (trigamma) were calculated with the package *MuMIn* (version 1.48.19) (Bartoń, 2026). The package *DHARMa* (version 0.4.7) (Hartig, 2024) was used for model diagnostics. The full and reduced models for the weaning group's cecal ASVs showed departure from the expected distribution of scaled residuals ($p = 0.031$), and the full (but not reduced) model significant quantile deviation ($p = 0.020$). The reduced model for post-recovery group's cecal ASVs had significant quantile deviation in the full model ($p = 0.029$), as well as the reduced model ($p = 0.025$). I attempted to address this by switching distributions and link-functions. While no alternative solutions fixed the problem, any reasonable alternative fits resulted in

similar results as the present model and did not alter conclusions drawn from the models.

Linear mixed models were fit to Shannon diversity using package *lme4* (version 2.0.1) (Bates et al., 2015) and *lmerTest* (version 3.2.1) (Kuznetsova et al., 2017), with sex, *C. innocuum* presence, and the interaction of maternal diet and selection direction as the fixed effects and litter ID nested in parallel line as random intercept. The significance of the interaction term was tested using ANOVA as above. To address singular fits, the nested random intercept was simplified as above.

To examine differences in community composition, I calculated the beta diversity metrics Bray-Curtis, Unweighted UniFrac and UniFrac for the post-recovery and weaning-aged pups cecal and fecal samples using R package *vegan* (version 2.7.3) (J. Oksanen et al., 2026). Bray-Curtis only accounts for relative abundance of taxa, Unweighted UniFrac for the presence/absence of taxa and their phylogenetic distance, and Weighted UniFrac weights phylogenetic distance based on abundance. I tested the differences in community composition between treatment and selection groups by fitting PERMANOVA models to the different dissimilarity metrics using the R package *vegan* (version 2.7.3) (J. Oksanen et al., 2026). PERMANOVA does not handle random effects natively, so they have to be incorporated by restricting permutations with an appropriate permutation scheme based on the experimental design (Anderson, 2017; Anderson & Braak, 2003). Unfortunately, in this experimental design, constructing a suitable permutation scheme to account for the random effects without losing the ability to test the focal interaction of selection direction and treatment was not feasible in the scope of this thesis, mainly because of restricted permutation options due to unbalanced group sizes. As discussed by Anderson (2017), permuting the data incorrectly results in an incorrect P-value regardless of whether the F-statistic is calculated correctly. Recognizing this caveat, I conducted freely permuting marginal PERMANOVA with 999 permutations for weaning-aged and post-recovery pups' cecal and fecal samples separately, with parallel line, sex, *C. innocuum* presence, and the focal interaction of maternal diet and selection direction as fixed effects. PERMANOVA assumes equal dispersion between groups because it does not distinguish between dispersion and the location of centroids in calculating P-values, so I tested multivariate

homogeneity of group dispersions in the model variables using the package *vegan* (version 2.7.3) (J. Oksanen et al., 2026). To visualize within-group differences to complement the PERMANOVA analyses, I ordinated each beta diversity metric in each group-sample type combination with the Principal Coordinate Analysis (PCoA) method using the package *phyloseq* (version 1.54.2) (McMurdie & Holmes, 2013).

2.5.4 Differential abundance

To identify taxa responsible for the possible differences between selection and treatment or their interaction, I conducted differential abundance analysis using ANCOMBC2 in the R package *ANCOMBC* (version 2.12.1) (Lin et al., 2022; Lin & Peddada, 2020, 2024) with multiple testing p-value adjustment with false discovery rate (FDR), pseudo positive value of 1, minimum prevalence in 5% of samples, minimum library size of 1000, level of significance at 0.05 and a maximum of 20 iterations. I modeled the interaction of treatment and selection while controlling for sex. Litter ID nested in parallel line was initially included as a random intercept. This resulted in a convergence failure in the model for weaning group's cecal samples, so I simplified the random intercept to parallel line for that model only. To examine the main effects of treatment and selection direction when the interaction was not significant, I fit reduced models without the interaction term. This again resulted in a convergence failure in the model for weaning group's cecal samples, so I had to exclude random effects entirely from this model.

ANCOMBC2 choice of pseudo positive value can sometimes affect the significance of results. This can be mitigated with built-in sensitivity analysis which tests with different pseudo-positives and marks the difference as robust if it passes these analyses. ANCOMBC2 developers recommend using sensitivity analysis, except in models where interactions are present, because the interaction term will not function properly (Lin, 2026). So, in primary models where the focal interaction of treatment and selection direction are present, the results were interpreted regardless of whether they passed sensitivity analysis. In reduced models without the interaction term, only the results that passed sensitivity analysis were regarded as significant.

3 Results

3.1 Effects of maternal diet on reproductive success and offspring growth

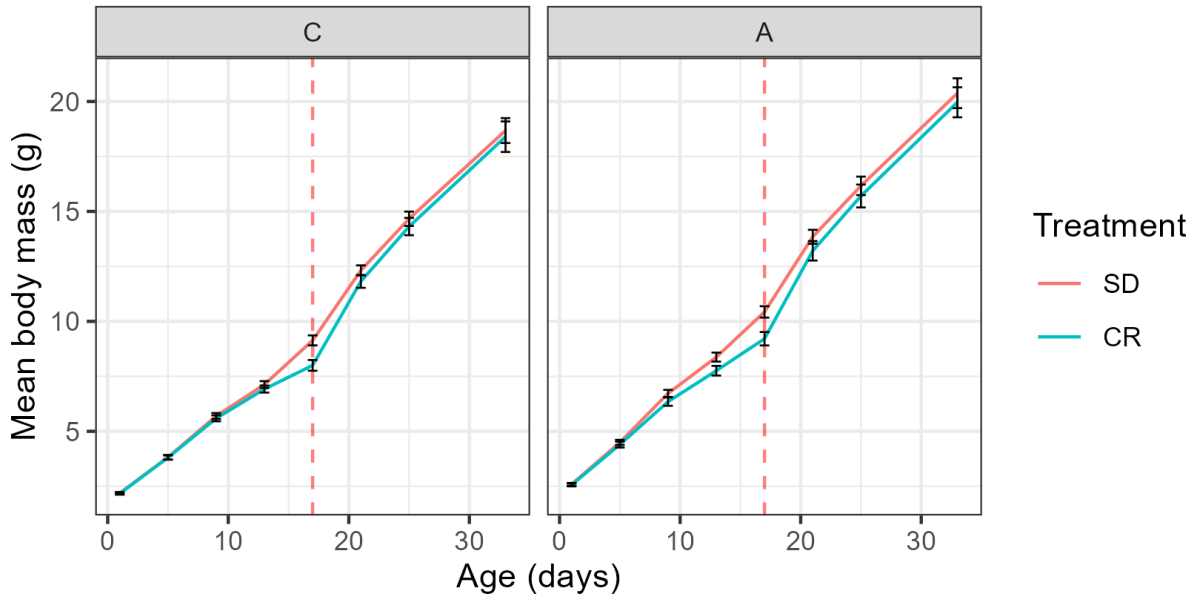

Figure 1 Bank vole pups' mean body mass over time with 95 % confidence intervals in control (C) and high metabolism (A) selection lines under standard (SD) and dietary restriction (CR) maternal diet. Weaning at the age of 17 days is marked with a vertical dashed line, which marks the beginning of the recovery period (all fed the standard diet).

No evidence was found for the hypothesis that the A-lines would suffer more from CR in terms of reproductive success or offspring growth (non-significant interactions of selection and treatment; Table 1). Neither selection nor maternal diet influenced litter size at weaning (main effects non-significant; Table 1E). In the offspring, maternal CR was associated with growth retardation in terms of mean body mass towards the end of nursing, with the most prominent difference at weaning in both selection directions, but this appeared to be compensated by catch-up growth as the pups entered the recovery period (Figure 1). Maternal diet had no effect on body mass at birth, but A-line pups were bigger at this stage (SelectionA estimate = 0.401 SE = 0.087, t(5.607) = 4.607, p = 0.004; Table 1A). At weaning, maternal CR decreased body mass similarly in both selection directions (TreatmentCR estimate = -0.745, SE = 0.251, t(85.252) = -2.963, p = 0.004) (Table 1B). A similar effect was observed in head width (a proxy for structural size), which was lower in pups who had experienced maternal CR (TreatmentCR estimate = -0.197, SE = 0.069, t(87.559) = -2.849, p = 0.005; Table 1D). The A-line pups

were larger than at weaning in terms of body mass (SelectionA estimate = 1.343, SE = 0.377, t(5.461) = 3.563, p = 0.014; Table 1B), and head width (SelectionA estimate = 0.412, SE = 0.095, t(5.292) = 4.315, p = 0.007; Table 1D). After the recovery period, however, no significant differences in body mass in response to selection, treatment or their interaction were observed (Table 1C). Taken together, these results indicate that the CR diet does not influence the dams' reproductive success in either selection direction, the effects of CR on pup growth emerge during the nursing period but do not result in permanent growth retardation, and that despite their early investment in growth, the A-lines are not disproportionately affected by CR in comparison to the C-lines.

Table 1 Linear mixed models (Satterthwaite degrees of freedom) fit to (A) pup body mass at birth, (B) weaning, and (C) after the recovery period, as well as (D) head width at weaning, Additionally, (E) litter size at weaning was modeled with a generalized linear mixed model with the Conway-Maxwell Poisson distribution. The interaction of selection and treatment was tested using ANOVA in linear mixed models, and a type III F-test on the estimated marginal means in generalized linear mixed models and dropped from the final model if non-significant to examine the main effects. Significant p-values (< 0.05) are in bold.

Response:	**A. Body mass 1 day after birth**					**B. Body mass at weaning (D17)**				
Treatment:Selection	**F**	**Df1**	**Df2**	**P**		**F**	**Df1**	**Df2**	**P**	
Interaction	0.006	1	89.765	0.936		0.046	1	84.046	0.830	
Fixed effects	**Estimate**	**SE**	**t**	**Df**	**P**	**Estimate**	**SE**	**t**	**Df**	**P**
(Intercept)	2.634	0.109	24.204	42. 246	< 0.001	11.900	0.483	24.645	44.419	< 0.001
SelectionA	0.401	0.087	4.607	5.607	**0.004**	1.343	0.377	3.563	5.461	**0.014**
TreatmentCR	0.035	0.049	0.720	91.274	0.473	-0.745	0.251	-2.963	85.252	**0.004**
SexMale	0.033	0.021	1.543	426.997	0.124	0.043	0.063	0.681	405.672	0.497
Litter Size	-0.089	0.017	-5.113	110.784	**< 0.001**	-0.555	0.081	-6.808	90.886	**< 0.001**
Random effects	**Std.Dev.**	**N**				**Std.Dev.**	**N**			
LitterID:Line	0.214	101				1.179	101			
Line	0.103	8				0.406	8			
Residual	0.213					0.404				
N	496					504				
R^2 marginal	0.334					0.389				
R^2 conditional	0.702					0.874				
Response:	**C. Body mass after recovery (D33)**					**D. Head width at weaning**				
Treatment:Selection	**F**	**Df1**	**Df2**	**P**		**F**	**Df1**	**Df2**	**P**	
Interaction	0.158	1	73.02	0.692		0,011	1	86.283	0,918	
Fixed effects	**Estimate**	**SE**	**t**	**Df**	**P**	**Estimate**	**SE**	**t**	**Df**	**P**
(Intercept)	17.069	0.822	20.772	6.580	< 0.001	12.079	0.133	91.160	53.948	< 0.001
SelectionA	1.831	1.135	1.614	5.978	0.158	0.412	0.095	4.315	5.292	**0.007**
TreatmentCR	-0.183	0.344	-0.534	74.074	0.595	-0.197	0.069	-2.849	87.559	**0.005**
SexMale	2.565	0.207	12.392	212.170	**< 0.001**	0.015	0.025	0.608	419.609	0.544
Litter Size						-0.102	0.023	-4.441	98.547	< 0.001

Random effects	**Std.Dev.**	**N**			**Std.Dev.**	**N**
LitterID:line	1.303	99			0.314	101
Line	1.532	8			0.095	8
Residual	1.741				0.252	
N	306				504	
R^2 marginal	0.274				0.303	
R^2 conditional	0.688				0.741	
Response:	**E. Litter size at weaning**					
Treatment:Selection	**X^2**	**Df**	**P**			
Interaction	0.29	1	0.692			
Fixed effects	**Estimate**	**SE**	**z**	**P**		
(Intercept)	1.553	0.073	21.395	< 0.001		
SelectionA	-0.012	0.086	-0.142	0.887		
TreatmentCR	0.005	0.086	0.063	0.949		
Random effects	**Std.Dev.**	**N**				
Line	< 0.001	8				
Residual						
N	107					
R^2 marginal	< 0.001					
R^2 conditional	<0.001					

3.2 Food consumption and digestible energy intake

To evaluate the capacity of the bank voles to compensate for the reduction of food quality by increasing their food intake, and thus, the efficacy of the diet treatment, we compared the quantity and caloric content consumed by the voles in different treatments and selection directions. The effects of CR on food consumption were similar in both selection directions (non-significant interaction of selection and treatment; Table 2 A-B). The A-line dams ate more than the C-line dams during nursing in both treatments (SelectionA estimate = 1.020, SE = 0.305, t(97.603) = 3.346. p = 0.001), and CR increased the mother's daily food consumption similarly in both selection directions (2.589, SE = 0.585, t(5.855) = 4.425, p = 0.005) (Table 2A). Maternal CR did not influence the pups' daily food consumption at the end of the recovery period, but A-lines still consumed more food (SelectionA estimate = 0.884, SE = 0.157, t(5.819) = 5.625, p = 0.001) (Table 2B).

Table 2 The linear mixed models (with Satterthwaite's method for estimating degrees of freedom) fit to (A) the dam's average food consumption on the experimental diet during lactation on days 9-13 after the birth of the litter, and (B) the pup's average food consumption at the end of the recovery period on standard diet, on days 25-33 after birth

Response:	**A. Dam average food consumption D9-13**					**B. Pup average food consumption D25-33**				
Treatment:Selection	**F**	**Df1**	**Df2**	**P**		**F**	**Df1**	**Df2**	**P**	
Interaction	0.061	1	96.545	0.805		0.013	1	88.984	0.908	
Fixed effects	**Estimate**	**SE**	**t**	**Df**	**P**	**Estimate**	**SE**	**t**	**Df**	**P**
(Intercept)	5.125	0.592	8.659	22.780	< 0.001	4.188	0.133	31.536	11.853	<0.001
TreatmentCR	1.020	0.305	3.346	97.603	**0.001**	0.159	0.140	1.132	90.074	0.261
SelectionA	2.589	0.585	4.425	5.855	**0.005**	0.884	0.157	5.625	5.819	**0.001**
Litter Size	0.914	0.083	10.962	95.791	**< 0.001**					
SexMale						0.416	0.075	5.517	260.140	**<0.001**
Random effects	**Std.Dev.**	**N**				**Std.Dev.**	**N**			
LitterID:Line	*					0.586	99			
Line	0.708	8				0.102	8			
Residual	1.528					0.668				
N	105					344				
R^2 marginal	0.618					0.389				
R^2 conditional	0.686					0.874				

* The effect not included in the model due to a singular fit

Although dams on the CR diet ate more than dams on the SD diet, they could not fully compensate for the decreased soluble energy density in CR food: Based on estimated marginal means of selection and treatment combinations (Table 3) and the soluble energy content in each experimental diets (SD: 14.37, CR: 9.86 KJ/g), estimated daily energy intake in the CR treatment was 24 % and 25 % lower in the C-lines and A-lines, respectively.

Table 3 Estimated marginal means of maternal food consumption on days 9-13 after the birth of the focal litter in dams of either control (C) or high metabolism (A) selection, on either standard diet (SD) or calorie-restricted diet (CR)

Treatment	Selection	emmean	SE	Df	95 % CI
SD	C	9.547	0.457	8.615	8.507 - 10.588
CR	C	10.494	0.476	9.683	9.429 - 11.56
SD	A	12.063	0.477	10.099	11.002 - 13.124
CR	A	13.161	0.469	9.457	12.108 - 14.215

3.3 Offspring's microbiota's response to maternal CR in different selection directions

3.3.1 Description of the relative abundance of bacterial phyla in bank vole gut microbiota

In unrarefied data, in total 25 distinct bacterial phyla were identified in the weaning and post-recovery group's cecum and the post-recovery group's feces (Figure 2). Overall, in the weaning group's cecum, *Bacillota* was the most abundant phylum (60.3 %) followed by *Bacteroidota* (28.0 %), and *Spirochaetota* (3.3 %). In the post-recovery group's cecum, *Bacillota* was also the most abundant (46.8 %), followed by *Bacteroidota* (21.6 %), and *Spirochaetota* (14.3 %). In the post-recovery group's feces *Bacillota* was overall the most abundant phylum (43.0 %), followed by *Bacteroidota* in nearly equal proportion (42.9 %), and *Actinomycetota* (4.3 %). (Data not shown).

Based on a visual inspection of the qualitative changes in relative abundances of phyla among treatments (Figure 2), in the weaning group's cecum, CR was associated with a relative increase in the proportion of *Bacteroidota*, and a decrease in *Actinomycetota* in both selection directions. In the post-recovery group's cecum, maternal CR was associated with a slight relative increase in *Bacillota*. In the post-recovery group's feces, the relative abundance of *Actinomycetota* was lower in the CR treatment in both selection directions, and the CR treatment was associated with higher relative abundance of *Bacillota* in the A-lines, but not the C-lines (Figure 2).

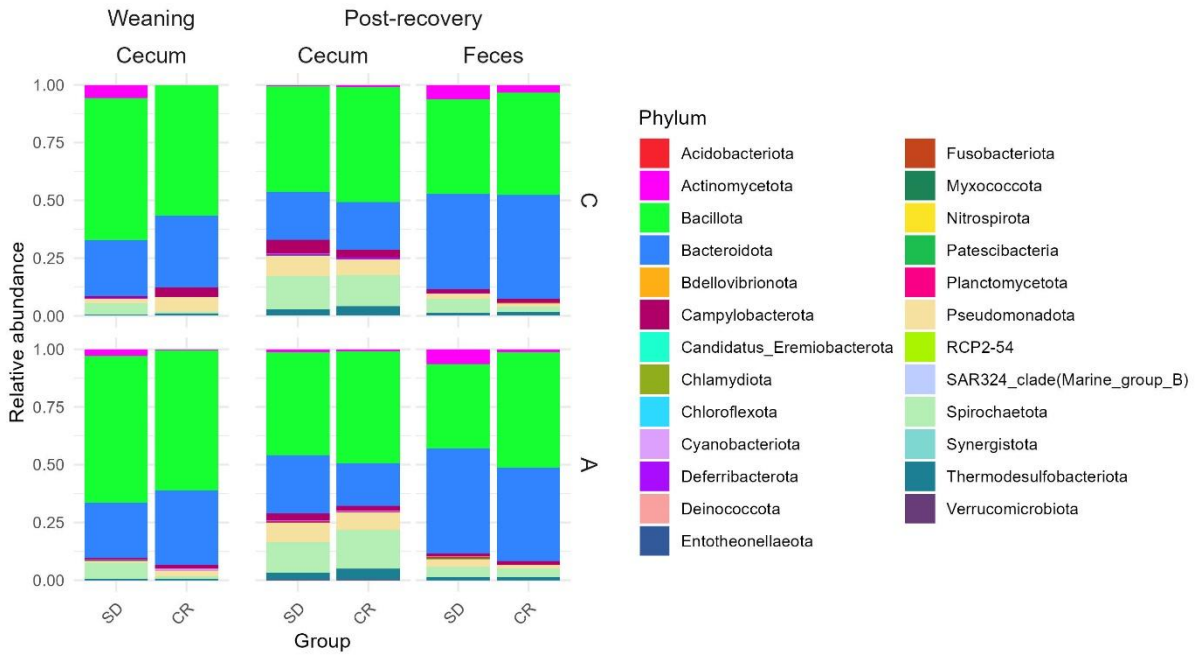

Figure 2 Relative abundance of bacterial phyla in pups belonging to either control (C) or high metabolism (A) lines, with either standard (SD) or restricted (CR) maternal diet at weaning (age 17 days) and after the recovery period (age 33 days). Relative abundance in cecal and fecal microbiota are plotted separately.

3.3.2 Alpha diversity

Contrary to my predictions, the responses to maternal CR in terms of microbiota species richness (observed ASVs) and Shannon index were similar in both selection directions in all groups and sample types (non-significant interaction of selection and treatment) (Table 4). The main effects of selection and maternal diet on observed ASVs were also non-significant in all groups and sample types (Table 4A-C). Selection direction had no significant effect on cecal microbiota Shannon index in the weaning or post-recovery groups (Table 4D-E). Maternal CR increased cecal Shannon index in the weaning group's (TreatmentCR estimate = 0.521, SE = 0.190, t(76.989) = 2.748, p = 0.007) (Table 4D), but no significant effect was observed the post-recovery group's cecum (Table 4E). In the post-recovery group's fecal microbiota, maternal diet had no effect on Shannon index, but it was higher in the A-lines (SelectionA estimate = 0.161, SE = 0.080, t(84.210) = 2.019, p = 0.047) (Table 4F). The different findings from ASV (richness) and Shannon index (richness adjusted for evenness) suggest that diet treatment did not impact the number of distinct taxa but caused a reversible change in the community structure. The increase in Shannon index implies a shift in the relative

abundances of taxa, with the community becoming more evenly distributed rather than dominated by a few abundant taxa.

Table 4 (Generalized) Linear mixed models fit to alpha diversity metrics (observed ASVs, Shannon index) in the weaning and post-recovery group's cecal microbiota and the post-recovery group's fecal microbiota. (A-C) Generalized linear mixed models with the negative binomial distribution fit to observed ASVs (D-F) Linear mixed models with Satterthwaite method for estimating degrees of freedom fit to Shannon index. Significant p-values (< 0.05) are in bold.

Response:	**A. Observed ASVs (weaning cecum)**					**B. Observed ASVs (post-recovery cecum)**				
Treatment:Selection	**X^2**	**Df**	**P**			**X^2**	**Df**	**P**		
Interaction	0.001	1	0.977			0.038	1	0.845		
Fixed effects	**Estimate**	**SE**	**z**	**P**		**Estimate**	**SE**	**z**	**P**	
(Intercept)	6.119	0.070	87.756	< 0.001		6.284	0.083	75.629	< 0.001	
TreatmentCR	0.035	0.063	0.553	0.581		0.056	0.056	0.998	0.318	
SelectionA	0.023	0.062	0.362	0.717		0.023	0.101	0.225	0.822	
SexMale	-0.023	0.064	-0.366	0.714		-0.093	0.055	-1.706	0.088	
C. innocuumPresent	0.010	0.066	0.148	0.883		-0.283	0.057	-4.935	**< 0.001**	
Random effects	**Std.Dev.**	**N**				**Std.Dev.**	**N**			
LitterID:Line	0.067	68				< 0.001	72			
Line	*					0.118	8			
Residual										
N	82					141				
R^2 marginal	0.007					0.169				
R^2 conditional	0.062					0.262				
Response:	**C. Observed ASVs (post-recovery feces)**					**D. Shannon index (weaning cecum)**				
Treatment:Selection	**X^2**	**Df**	**P**			**F**	**Df1**	**Df2**	**P**	
Interaction	1.791	1	0.181			0.027	1	75.987	0.871	
Fixed effects	**Estimate**	**SE**	**z**	**P**		**Estimate**	**SE**	**t**	**Df**	**P**
(Intercept)	5.982	0.052	115.598	< 0.001		3.668	0.213	17.207	25.872	< 0.001
TreatmentCR	-0.003	0.049	-0.056	0.955		0.521	0.190	2.748	76.989	**0.007**
SelectionA	0.078	0.049	1.582	0.114		0.116	0.201	0.576	5.761	0.586
SexMale	-0.069	0.031	-2.269	**0.023**		0.047	0.194	0.242	74.442	0.809
C. innocuumPresent	-0.071	0.040	-1.788	0.074		0.062	0.198	0.313	72.711	0.755
Random effects	**Std.Dev.**	**N**				**Std.Dev.**	**N**			
LitterID:line	0.185	95				*				
Line	< 0.001	8				0.094	8			
Residual						0.851				
N	259					82				
R^2 marginal	0.036					0.091				
R^2 conditional	0.400					0.102				
Response:	**E. Shannon index (post-recovery cecum)**					**F. Shannon index (post-recovery feces)**				
Treatment:Selection	**F**	**Df1**	**Df2**	**P**		**F**	**Df1**	**Df2**	**P**	
Interaction	0.321	1	58.721	0.573		0.066	1	82.386	0.798	
Fixed effects	**Estimate**	**SE**	**t**	**Df**	**P**	**Estimate**	**SE**	**t**	**Df**	**P**
(Intercept)	3.984	0.193	20.681	15.214	< 0.001	3.177	0.090	35.145	149.031	< 0.0001
TreatmentCR	-0.068	0.146	-0.466	135.931	0.642	0.124	0.079	1.557	83.118	0.123

SelectionA	-0.199	0.213	-0.931	5.894	0.388	0.161	0.080	2.020	84.210	**0.047**
SexMale	-0.211	0.143	-1.478	132.514	0.142	-0.118	0.065	-1.825	194.348	0.069
C. innocuumPresent	-0.384	0.146	-2.627	135.694	**0.010**	-0.015	0.075	-0.195	226.821	0.846
Random effects	**Std.Dev.**	**N**				**Std.Dev.**	**N**			
LitterID:Line	*					0.228	95			
Line	0.222	8				*				
Residual	0.833					0.504				
N	141					259				
R^2 marginal	0.072					0.042				
R^2 conditional	0.139					0.206				

* Random effects simplified due to a singular fit

3.3.3 Beta diversity

To assess whether the offspring's microbial community responds distinctly to maternal CR at weaning and after recovery depending on selection direction, PERMANOVA models were fit to the dissimilarity metrics Bray-Curtis, weighted UniFrac and unweighted UniFrac in each group and sample type, testing the focal interaction of treatment and selection. First, I evaluated the PERMANOVA assumption of equal dispersions between the levels of each variable included in the models, and found that this assumption was violated in some models: In the weaning-aged pups' cecal microbiota, Weighted UniFrac group dispersions differed significantly in treatment ($p = 0.009$; Table 5A), which is also visible in the 95 % confidence ellipses around treatment of the corresponding PCoA ordination in Figure 3C. In the recovery group's fecal samples, Weighted UniFrac group dispersion was significantly different in treatment ($p = 0.004$), *C. innocuum* presence ($p = 0.048$), sex ($p = 0.030$), and parallel line ($p = 0.002$), and Bray-Curtis and Unweighted UniFrac in *C. innocuum* presence ($p = 0.005$) (Table 5C). Current methods offer limited means to address this issue. Thus I advise caution in interpreting the reported model results.

Table 5 The results of multivariate group dispersion (Betadisper) test for each beta diversity metric and sample type. Statistically significant p-values (< 0.05) of variables that have significantly different group dispersions (violate model assumptions) are in bold. BC is short for Bray-Curtis, UUF for Unweighted UniFrac, and WUF for Weighted UniFrac.

	A. Betadisper weaning cecum			B. Betadisper recovery cecum			C. Betadisper recovery feces		
Dissimilarity metric:	**BC**	**UUF**	**WUF**	**BC**	**UUF**	**WUF**	**BC**	**UUF**	**WUF**
Variable	**p**	**p**	**p**	**p**	**p**	**p**	**p**	**p**	**P**
Treatment	0.243	0.549	**0.009***	0.994	0.051	0.327	0.118	0.885	**0.004***
Selection	0.472	0.826	0.223	0.561	0.434	0.359	0.977	0.399	0.197
C. innocuum presence	0.429	0.341	0.507	0.127	0.484	0.096	**0.007***	**0.004***	**0.048***
Sex	0.415	0.982	0.213	0.370	0.829	0.701	0.177	0.183	**0.030***
Parallel line	0.629	0.979	0.508	0.242	0.444	0.911	0.315	0.347	**0.002***

* Variables that have significantly different group dispersions (violate model assumptions).

In partial support of my hypothesis, the cecum microbiota of weaning-aged pups from the two selection directions responded differently to the dietary treatment, indicated by a statistically significant the interaction of treatment and selection in the phylogenetically informed diversity metrics Unweighted UniFrac (R^2 = 0.016, F = 1.346, p = 0.038; Table 6A-II) and Weighted UniFrac (R^2 = 0.021, F = 1.957, P = 0.031; Table 6A-III) but not Bray-Curtis (Table 6A-I). The principal coordinates used to visualize the beta diversity (Figure 3) show clear differentiation of diet treatments, with much subtler differences seen for selection directions. As mentioned above, the dispersions differ among groups, which influences the interpretation of model results. Notably, the samples from CR treatment in both Bray-Curtis and Weighted UniFrac cluster closely together, indicating that the communities within CR treatment were more similar to each other compared to a higher heterogeneity in cecum samples from SD treatment.

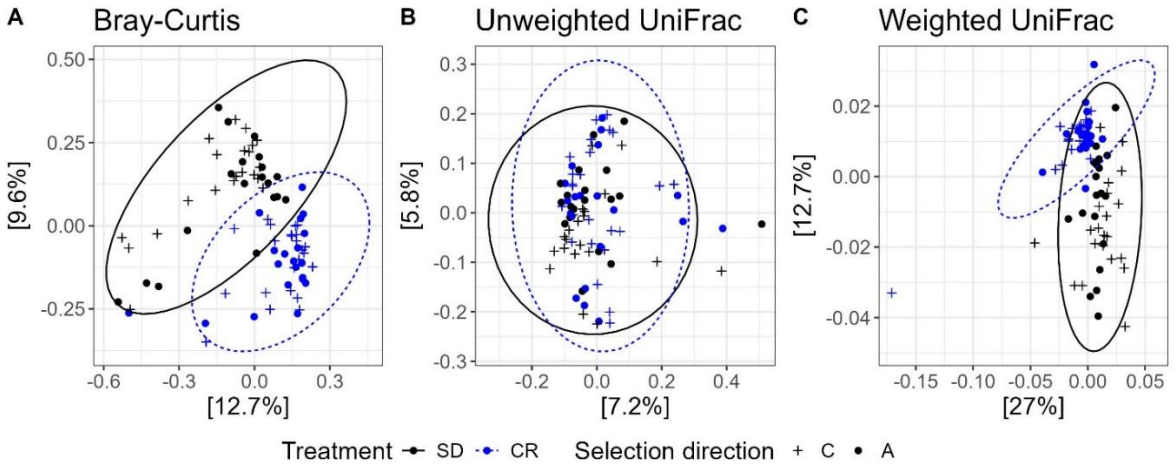

Figure 3 Beta diversity of cecal microbiota in the weaning-aged pups visualized in PCoA in the dissimilarity metrics (A) Bray-Curtis (B) Unweighted UniFrac and (C) Weighted UniFrac. 95 % confidence ellipses drawn around treatment.

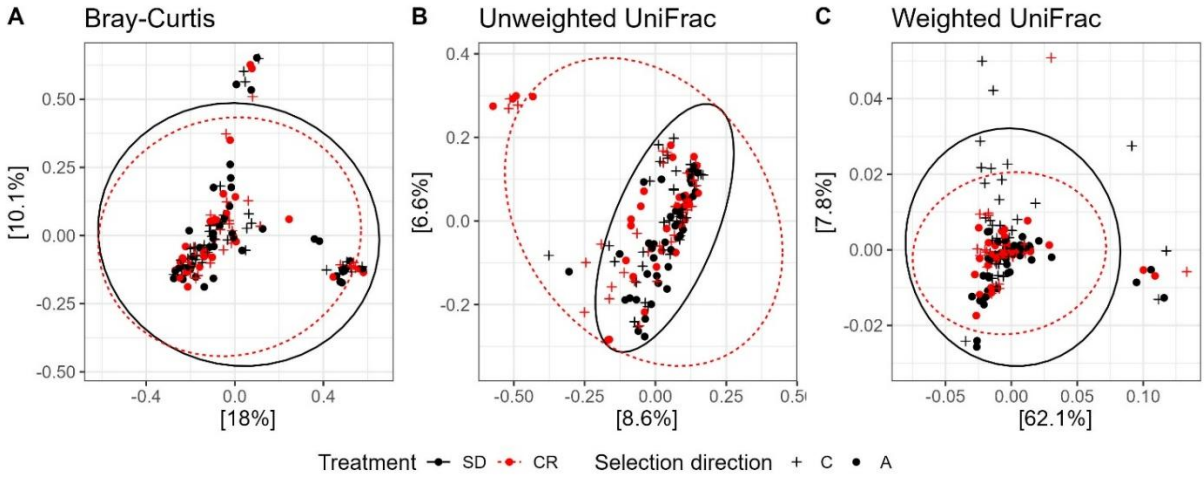

Figure 4 Beta diversity of cecal microbiota in the post-recovery pups visualized in PCoA in the dissimilarity metrics (A) Bray-Curtis (B) Unweighted UniFrac and (C) Weighted UniFrac. 95 % confidence ellipses drawn around treatment.

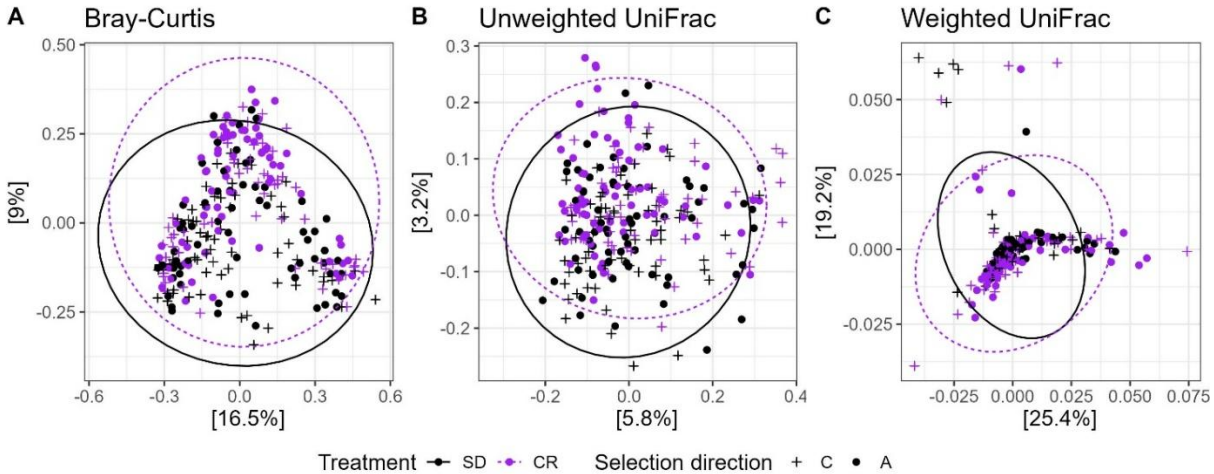

Figure 5 Beta diversity of fecal microbiota in the post-recovery pups visualized in PCoA in the dissimilarity metrics (A) Bray-Curtis (B) Unweighted UniFrac and (C) Weighted UniFrac. 95 % confidence ellipses drawn around treatment.

Table 6 Results of marginal PERMANOVA models fit to the beta diversity metrics I. Bray-Curtis, II. Unweighted UniFrac and III. Weighted UniFrac in the microbiota of (A) weaning group's cecum, (B) recovery group's cecum, and (C) recovery group's feces.

		A. PERMANOVA Weaning Cecum											
		I. Bray-Curtis				II. Unweighted UniFrac				III. Weighted UniFrac			
Term	**Df**	**SS**	**R^2**	**F**	**p**	**SS**	**R^2**	**F**	**p**	**SS**	**R^2**	**F**	**p**
Parallel line	6	1.973	0.079	1.202	0.034	1.200	0.077	1.088	0.085	0.012	0.071	1.119	0.247
C. innocuum presence	1	0.388	0.016	1.420	0.056	0.332	0.021	1.807	**0.001**	0.002	0.012	1.131	0.307
Sex	1	0.224	0.009	0.818	0.757	0.140	0.009	0.760	0.967	0.002	0.012	1.124	0.311
Treatment:Selection	1	0.352	0.014	1.285	0.130*	0.247	0.016	1.346	**0.038**	0.004	0.021	1.957	**0.031**
Residual	71	19.420	0.779			13.047	0.836			0.131	0.749		
Total	82	24.933	1.000			15.601	1.000			0.175	1.000		
		B. PERMANOVA Recovery Cecum											
		I. Bray-Curtis				II. Unweighted UniFrac				III. Weighted UniFrac			
Term	**Df**	**SS**	**R^2**	**F**	**p**	**SS**	**R^2**	**F**	**p**	**SS**	**R^2**	**F**	**p**
Parallel line	6	3.457	0.072	1.900	**0.001**	2.154	0.057	1.403	**0.002**	0.012	0.056	1.410	0.123
C. innocuum presence	1	2.264	0.047	7.467	**0.001**	1.031	0.027	4.027	**0.001**	0.009	0.039	5.904	**0.004**
Sex	1	0.471	0.010	1.554	0.062	0.221	0.006	0.864	0.796	0.002	0.009	1.385	0.207
Treatment:Selection	1	0.258	0.005	0.850	0.604	0.304	0.008	1.188	0.123	0.001	0.006	0.879	0.399
Residual	130	39.416	0.825			33.277	0.876			0.188	0.853		
Total	141	47.787	1.000			37.973	1.000			0.221	1.000		
		C. PERMANOVA Recovery Feces											
		I. Bray-Curtis				II. Unweighted UniFrac				III. Weighted UniFrac			
Term	**Df**	**SS**	**R^2**	**F**	**p**	**SS**	**R^2**	**F**	**p**	**SS**	**R^2**	**F**	**p**
Parallel line	6	3.489	0.046	2.151	**0.001**	2.607	0.038	1.691	**0.001**	0.015	0.066	3.049	**0.001***
C. innocuum presence	1	1.501	0.020	5.551	**0.001***	0.949	0.014	3.691	**0.001***	0.003	0.011	3.161	**0.005***
Sex	1	0.368	0.005	1.361	0.136	0.246	0.004	0.958	0.609	0.000	0.002	0.532	0.852*
Treatment:Selection	1	0.698	0.009	2.581	**0.003**	0.397	0.006	1.545	**0.001**	0.002	0.007	2.064	**0.037***
Residual	249	67.312	0.887			64.002	0.922			0.206	0.900		
Total	260	75.875	1.000			69.420	1.000			0.229	1.000		

* Term or its constituent associated with model violations as reported in Table 5.

The interaction of treatment and selection was not significant in the post-recovery pups' cecal microbiota in any of the beta diversity metrics (Table 6B). This is consistent with the PCoA plots (Figure 4), which show largely overlapping clustering of the samples from different selection and treatment groups. Significant main effects of parallel line and *C. innocuum* presence (Table 6B-I, II) may contribute to separation unexplained by selection and treatment in the ordination plots of Bray-Curtis and Unweighted UniFrac (Figure 4A, B). In the post-recovery group's fecal microbiota, however, the interaction of treatment and selection was significant in Bray-Curtis (R^2 = 0.009, F = 2.581, p = 0.003) (Table 6B-I), Unweighted UniFrac (R^2 = 0.006, F = 1.545, p = 0.001) (Table 6B-II), and Weighted UniFrac (R^2 = 0.007, F = 2.064, p = 0.037) (Table 6B-III), which suggests a weak

sustained selection-specific response in the gut bacterial community composition as a whole. The interaction is not distinguishable or captured by the first ordination axes in the corresponding PCoA plots, but a shift (with considerable overlap) between maternal diet groups can be seen in the ordination plots of Bray-Curtis (Figure 5C) and Unweighted UniFrac (Figure 5C).

3.3.4 Differential abundance

Differential abundance analysis was conducted to identify genera with a response in relative abundance to the interaction of treatment and selection or their main effects. In contrast with my predictions, the interaction of treatment and selection was non-significant (FDR-adjusted significance, $q > 0.05$) in all bacterial genera in the weaning and post-recovery group's cecum as well as the post-recovery group's feces, suggesting a similar response to CR in both selection directions. The main effect of selection was also non-significant for all genera in all groups and sample types. Maternal CR, however, resulted in 11 differentially abundant genera in the weaning group's cecum (TreatmentCR $q < 0.05$, passed sensitivity analysis; Figure 6). In the post-recovery group's cecum, no genera were differentially abundant in response to maternal CR. In the post-recovery group's feces, however, a genus of uncertain placement (*Incertae Sedis*) within the family *Christensenellaceae* decreased in response to maternal CR (LFC – 1.201, $q = 0.025$).

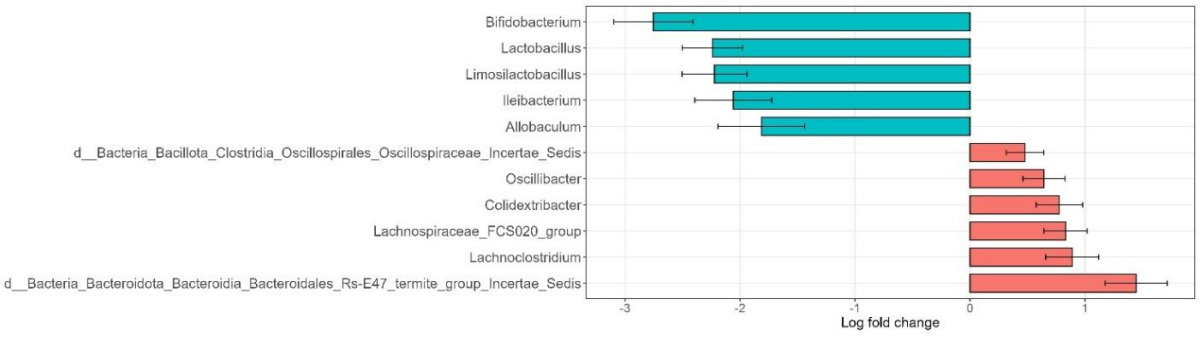

Figure 6 Log fold change (LFC) of the significant differentially abundant genera in the weaning group's cecum in response to the maternal dietary restriction compared with control diet. Negative LFC (decrease in abundance) is colored in blue and positive LFC (increase in abundance) is colored in red.

3.4 Cecal SCFA concentration after the recovery period

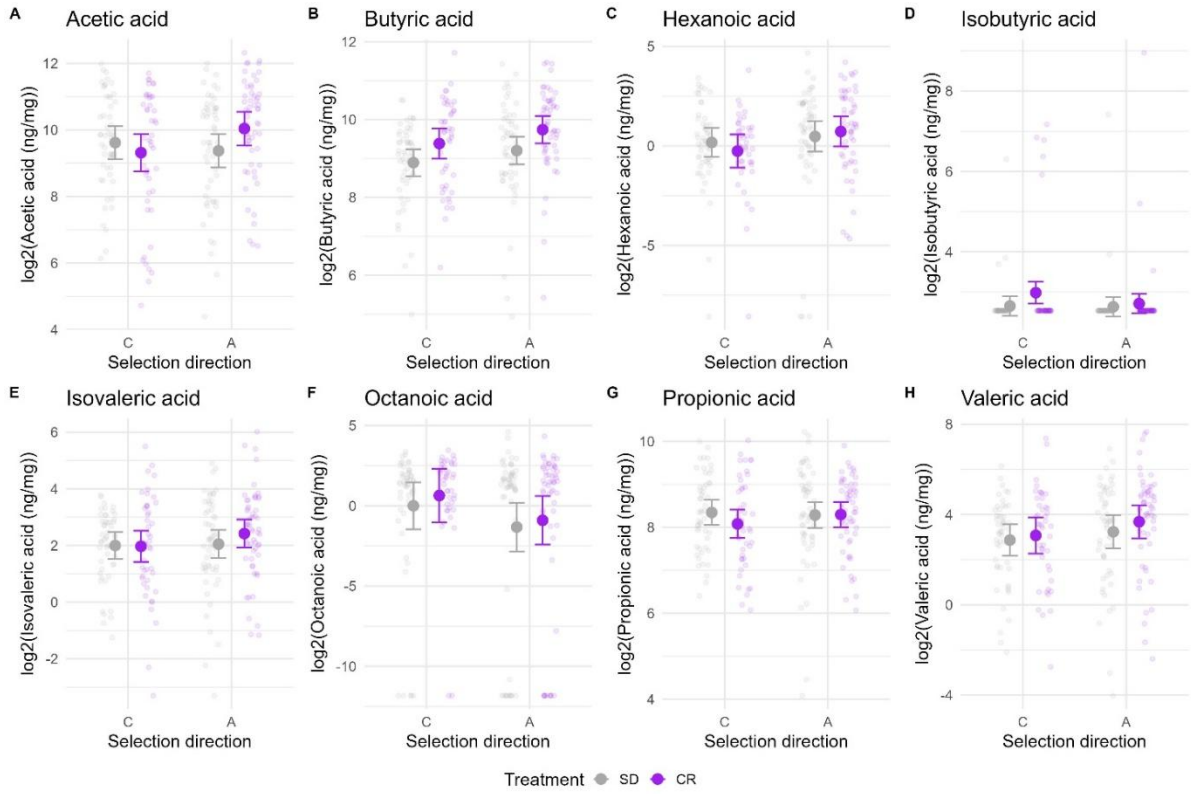

Figure 7 Estimated marginal means of the full models containing the interaction of selection and treatment fit to log2-transformed SCFA concentrations with 95 % confidence intervals. Log2-transformed data is plotted in the background.

I found limited support for persistent effects in the metabolite profile of cecum content of the post-recovery pups, as only one (butyrate) of the eight quantified SCFAs showed any response to selection or treatment. The interaction of selection and treatment was non-significant in all SCFAs, and the main effects of selection and treatment in most SCFAs (Table 7; Figure 7), except for butyrate (butyric acid), whose concentration was elevated in response to maternal CR in both selection directions (TreatmentCR estimate = 0.517, SE = 0.179, t(70.648) = 2.880, p = 0.005) (Table 7B; Figure 7B).

Table 7 Linear mixed models (with Satterthwaite's method for estimating degrees of freedom) fit to log2-transformed concentrations of eight SCFAs (A-H) in the offspring cecum after the recovery period. Significant p-values (< 0.05) are in bold.

Response	**A. Acetic acid**					**B. Butyric acid**				
Treatment:Selection		**Df1**	**Df2**	**F**	**P**		**Df1**	**Df2**	**F**	**P**
Interaction		1	73.191	3.506	0.065		1	70.320	0.017	0.895
Fixed effects	**Estimate**	**Std. Error**	**t**	**Df**	**P**	**Estimate**	**Std. Error**	**t**	**Df**	**P**
(Intercept)	9.545	0.249	38.389	128.862	< 0.001	8.979	0.171	52.567	126.373	< 0.001
TreatmentCR	0.208	0.265	0.785	78.179	0.435	0.517	0.179	2.880	70.648	**0.005**

SelectionA	0.202	0.265	0.762	79.206	0.448	0.332	0.180	1.847	71.731	0.069
SexMale	-0.297	0.211	-1.402	150.480	0.163	-0.196	0.151	-1.299	148.483	0.196
Random effects	**Std.Dev.**	**N**				**Std.Dev.**	**N**			
LitterID	0.770	94				0.469	94			
Residual	1.471					1.057				
N	210					210				
R2 marginal	0.015					0.074				
R2 conditional	0.227					0.227				
Response	**C. Hexanoic acid**					**D. Isobutyric acid**				
Treatment:Selection		**Df1**	**Df2**	**F**	**P**		**Df1**	**Df2**	**F**	**P**
Interaction		1	79.984	0.774	0.381		1	89.897	1.022	0.315
Fixed effects	**Estimate**	**Std. Error**	**t**	**Df**	**P**	**Estimate**	**Std. Error**	**t**	**Df**	**P**
(Intercept)	0.292	0.353	0.829	121.464	0.409	2.663	0.126	21.096	159.320	< 0.001
TreatmentCR	-0.081	0.386	-0.211	80.457	0.834	0.196	0.126	1.551	91.233	0.124
SelectionA	0.621	0.386	1.610	81.324	0.111	-0.140	0.126	-1.106	92.862	0.272
SexMale	-0.544	0.276	-1.969	144.184	0.051	0.104	0.123	0.849	175.598	0.397
Random effects	**Std.Dev.**	**N**				**Std.Dev.**	**N**			
LitterID	1.295	94				0.141	94			
Residual	1.896					0.882				
N	210					210				
R2 marginal	0.029					0.019				
R2 conditional	0.338					0.044				
Response	**E. Isovaleric acid**					**F. Octanoic acid**				
Treatment:Selection		**Df1**	**Df2**	**F**	**P**		**Df1**	**Df2**	**F**	**P**
Interaction		1	72.335	0.629	0.430		1	79.683	0.020	0.887
Fixed effects	**Estimate**	**Std. Error**	**t**	**Df**	**P**	**Estimate**	**Std. Error**	**t**	**Df**	**P**
(Intercept)	2.153	0.236	9.122	122.489	< 0.001	-0.174	0.710	-0.245	124.833	0.807
TreatmentCR	0.180	0.252	0.714	72.490	0.477	0.526	0.769	0.683	80.461	0.496
SelectionA	0.240	0.252	0.951	73.475	0.345	-1.427	0.770	-1.854	81.384	0.067
SexMale	-0.489	0.200	-2.447	145.044	**0.016**	0.444	0.574	0.774	147.058	0.440
Random effects	**Std.Dev.**	**N**				**Std.Dev.**	**N**			
LitterID	0.739	94				2.471	94			
Residual	1.390					3.955				
N	210					210				
R2 marginal	0.032					0.026				
R2 conditional	0.245					0.300				
Response	**G. Propionic acid**					**H. Valeric acid**				
Treatment:Selection		**Df1**	**Df2**	**F**	**P**		**Df1**	**Df2**	**F**	**P**
Interaction		1	69.262	0.824	0.367		1	78.660	0.102	0.750
Fixed effects	**Estimate**	**Std. Error**	**t**	**Df**	**P**	**Estimate**	**Std. Error**	**t**	**Df**	**P**
(Intercept)	8.380	0.147	57.173	130.015	< 0.001	3.181	0.331	9.611	110.570	< 0.001
TreatmentCR	-0.121	0.152	-0.797	69.283	0.428	0.329	0.371	0.885	79.388	0.379
SelectionA	0.070	0.152	0.459	70.464	0.648	0.480	0.371	1.293	80.105	0.200
SexMale	-0.197	0.134	-1.474	151.780	0.143	-0.731	0.233	-3.132	134.618	**0.002**
Random effects	**Std.Dev.**	**N**				**Std.Dev.**	**N**			
LitterID	0.347	94				1.391	94			
Residual	0.943					1.578				

N	210	210
R2 marginal	0.013	0.046
R2 conditional	0.131	0.463

4 Discussion

I hypothesized that the A-line voles with higher metabolic rate would suffer more from maternal calorie restriction but found no evidence for a greater impact of CR on the A-lines' reproductive success or offspring growth. While A-line pups were bigger at birth and weaning, consistent with previous observations in A-line adults (Hseiky et al., 2026; Lipowska et al., 2022, 2025), the effects of maternal CR were similar in both selection directions in all phases. CR had no effect on birth weight but influenced the growth of pups (structural size and body mass) to weaning age. The finding on birth weight is in contrast with previous literature, which has linked gestational undernutrition to low birth weight followed and increased propensity for obesity in adulthood in humans and rodents (Desai & Hales, 1997; Gilley et al., 2024). However, moderate caloric restriction during lactation lowers body mass (but not body length) at weaning, with a protective effect against obesity later in life in rodents (Palou et al., 2010). The effects of calorie restriction and the associated developmental outcomes for the offspring can thus depend on the timing of diet intervention, indicating multiple sensitive time windows for reprogramming. Here, the offspring experienced both, which may result in intermediate or net zero effects, if the programming at different time windows cancel each other out, or complex outcomes that are not captured here. Additionally, the severity of dietary intervention can engage distinct pathways (Liu et al., 2022). In mice, fetal growth restriction has previously been induced by 30 % reduction in food portions (Gilley et al., 2024), while here, food was diluted with 30 % cellulose and available *ad libitum*. Indeed, the dams compensated for reduced energy density by eating more during lactation. While the A-line dams ate more in both treatments, they did not excessively increase their food consumption in response to CR diet. However, physiological constraints such as gut size and food passage time may limit the capacity to increase food intake (Speakman & Król, 2005). Lactational calorie restriction applied to rats by Palou et al. (2010), similar in severity to the one used here, resulted in lower body mass at birth followed by decreased calorie intake later in life. In the present study, no lasting effects on maternal CR on the offspring's food consumption in either selection direction were observed. In summary, these results suggest that despite the greater investment in growth early in life as demonstrated by their larger size at birth and weaning, the A-lines

can adapt to caloric restriction with a similar efficiency as the C-lines, and that neither lines experience lasting effects in terms of body mass or food consumption.

We also hypothesized that the symbiotic microbiota may mediate phenotypic plasticity to a different capacity depending on selection direction to help the hosts meet their different energy needs early in life. Because maternal diet during gestation and lactation can have persistent effects on the offspring's metabolic phenotype (Desai & Hales, 1997; Palou et al., 2010), we assessed whether the effects on offspring microbiota also persist. Alpha diversity metrics did not provide evidence for selection-specific response to maternal CR: the effects on observed ASVs and Shannon index were similar in both selection lines in both weaning and recovery phases. Observed ASVs as a proxy for species richness did not differ between the selection directions or treatments at any phase, which is expected in a shared, enclosed environment, but also reflects the ability of the microbiota to retain phylogenetic diversity under changing dietary conditions early in life. Shannon diversity, which also accounts for species evenness, increased similarly in both selection directions in response to maternal CR at weaning. This reflects changes in community structure as an acute response to maternal CR. This may be mediated, in part, by diet-induced changes in the bacteria delivered to the offspring in milk during nursing (Martínez-Oca et al., 2023). These changes were reversible, as no difference associated with maternal CR was observed in cecal or fecal samples of the post-recovery group.

Unlike alpha diversity metrics, phylogenetically informed beta diversity metrics supported the hypothesis that cecal microbiota may respond distinctly to maternal CR in the different selection lines at weaning. Unweighted and Weighted UniFrac suggested a weak but significant selection-specific shift in the cecal microbiota in response to selection. Such signal may be indicative of a distinct bacterially mediated plasticity in the selection lines with different energy needs. However, no genera showed significant differential abundance for the interaction of treatment and selection in the cecum, nor were cecal SCFAs analyzed at this stage, so the functional consequences are practically unknown. Due to the weak effect size and functional redundancy prevalent in the gut microbiota (Doolittle & Booth, 2017), the effect may have limited biological relevance. The effect of maternal CR on cecal community composition was reversible,

as the interaction was non-significant in all beta diversity metrics in the post-recovery group's cecum, and the PCoA plots did not show any separation between the treatments. In the post-recovery group's feces, however, all beta diversity metrics signaled a weak, persistent effect that is distinct in each selection direction in response to CR. As in the weaning group's cecum, no genera were significantly differentially abundant in terms of the interaction. However, the PERMANOVA results' P-values should be interpreted with caution due to insufficiently accounted for pseudoreplication and due to violated model assumptions, as reported in sections 2.5.3 and 3.3.3.

All genera identified in the differential abundance analysis in the weaning group's cecum were in response to the main effect of maternal diet, and none were detected in the cecum of the post-recovery group, indicating that the changes induced by maternal diet are reversible. Majority of the affected genera in either direction belonged to *Firmicutes* (*Bacillota*), with one genus belonging to the phylum *Actinomycetota* among those that decreased, and one belonging to *Bacteroides* among those that increased in CR compared to SD. The genera with the most prominent decrease include *Bifidobacterium* (phylum *Actinomycetota*) and *Lactobacillus* (phylum *Bacillota*), who are important pioneers in the maturation of offspring's gut microbiota and are vertically transmitted from mother to child (Martino et al., 2022; Milani et al., 2017). Consistent with the findings here, a relative decrease in *Lactobacillus* and *Bifidobacterium* following gestational undernutrition has been observed in 4-week-old mice (Gilley et al., 2024). In contrast to this, Martìnez-Oca et al. (2023) reported increased abundance of *Bifidobacterium* in response to maternal undernutrition during gestation and lactation in mice. A negative association between maternal diet rich in fruit and vegetables and infant fecal Bifidobacteria abundance has been observed in humans (Lundgren et al., 2018), which may be adjacent to the increased proportion of dietary fiber in the present study. Members of the *Lactobacillus* genus are one of the earliest colonizers of infant gut, contributing to pathogen protection and oxygen depletion to make the gut habitable to anaerobes (Martino et al., 2022). The decrease in *Lactobacillus* in response to maternal CR may thus signal alterations in the maturation process of the cecal microbiota. The genus that increased the most in response to maternal CR was an

uncertainly placed genus in the *Rs-E47 termite group* family. This genus is not well characterized, but the *Rs-E47* have previously been reported to increase as *Lactobacillaceae* decreased in a diet manipulation experiment including gut-colonizing protozoa in mice (Wei et al., 2020). Though the experimental setting is different, this pattern is consistent with the one observed here. *Lachnoclostridium*, belonging to the family *Lachnospiraceae*, also increased in response to CR. The family contains major SCFA producers, but is functionally diverse, including also disease-related taxa in humans (Vacca et al., 2020). A decrease in butyrate-producing *Lachnospiraceae* has been linked to dysregulated lipid metabolism as a response to both maternal 50 % food restriction and a high-fat diet (Kim et al., 2025), but the calorie restriction was more severe than the one used here. As discussed above, the severity of calorie restriction may impact the outcomes for the host and the microbiota, and the findings here represent moderate rather than severe restriction, which may result in opposite metabolic outcomes (Palou et al., 2010). Members of the genus *Lachnoclostridium* include prominent butyrate producers (Gutiérrez & Garrido, 2019), but lacking species-level resolution and metabolomic data in the weaning group, the functional consequences of these changes are speculative.

Cecal SCFA quantities in the post-recovery group were similar in both selection directions. Maternal CR did not have lasting effects on the majority of measured SCFAs, including acetate and propionate. Cecal butyrate concentration, however, was elevated after the recovery period. Butyrate is beneficial to the health of the intestinal barrier (Donohoe et al., 2011) and contributes to regulation of appetite and insulin sensitivity, protecting the host from obesity and diabetes (Mayorga-Ramos et al., 2022). This may counteract adverse effects of gestational calorie restriction that can result in opposite outcomes in the offspring (Gilley et al., 2024), possibly mediated by sustained calorie restriction during the nursing period (Palou et al., 2010). The increase in cecal butyrate did not co-occur with any changes in bacterial diversity or community composition, nor were any differentially abundant genera identified in the cecum at this stage. The differences in bacterial metabolism may be explained by community differences below the resolution of those used here. Additionally, differential abundance analysis of the fecal bacterial community in the post-recovery group showed a decrease in one genus

belonging to the family *Christensenellacea* in response to maternal CR. The relative abundance of this family is inversely related to body mass index in humans (Waters & Ley, 2019). Together, these provide partial evidence that the effects of maternal CR in the wider context of the gut and bacterial metabolism may be lasting, with implications to metabolic phenotype protective of obesity and metabolic disorder.

In summary, the selection lines with different intrinsic energy requirements responded similarly to maternal calorie restriction in most aspects examined here. A-lines were not disproportionately affected by maternal calorie restriction despite their larger investment in early growth, suggesting plastic capacity that enables resource investment early in life. This was not associated with selection-specific responses to calorie restriction in alpha diversity or differential abundance, although beta diversity metrics suggested a weak but distinct community shift depending on selection. This provides limited evidence for the hypothesis that the microbiota differentially contributes to the modulation of phenotypic plasticity in metabolically diverged selection lines. Some irreversible effects of calorie restriction were observed in bacterial metabolism and community, but these indicated beneficial rather than detrimental effects on the offspring's metabolic health. The contrasting results in studies examining maternal calorie restriction may be explained, in part, by the severity and timing of dietary intervention.

While this study succeeded in clarifying the impact of maternal calorie restriction on the offspring and their microbiota, it nonetheless has a number of limitations that future work should aim to address. The functional characterization of the microbiota was limited: differential abundance analysis was done on the genus level, but many bacterial genera can be functionally diverse (Vacca et al., 2020), so functional consequences can only be estimated based on general characteristics of the taxon. Alpha and beta diversity may also be limited as proxies for functionally meaningful change because functional redundancy is common in the cut microbiota (Doolittle & Booth, 2017). In future work, shotgun metagenomics could provide better resolution into functional characterization of the microbiota. Because CR was based on dilution with cellulose which can be metabolized into SCFA by certain bacteria, measuring the residual cellulose concentration in the feces would provide information about the

cellulose utilization efficiency. Additionally, SCFAs provide a relatively narrow view of microbial metabolism in the gut. To expand on these findings, future work could include untargeted metabolomics to achieve a broader view of the microbiota's metabolome. Furthermore, physiological, genetic, and metabolomic data were analyzed separately here. Integrative analysis approaches could help better understand the mechanistic links between host physiology, microbiota community composition, and microbial metabolism.

5 Acknowledgements

The original project was funded by National Science Center OPUS 15 no. 2018/29/B/NZ8/01924 to Anni Hämäläinen. The base colony of the voles (the selection experiment) was funded from National Science Centre (2016/23/B/NZ8/00888 to Pawel Koteja), and the Jagiellonian University (project DS/WBINOZ/INOS/757).

I want to thank the supervisors, Anni Hämäläinen and Santosh Lamichhane for their continued support and insight during the making of this thesis, Pawel Koteja and his team for planning and executing the study, as well as the laboratory technicians and assistants who contributed to collecting the data.

References

Amato, K. R. (2013). Co-evolution in context: The importance of studying gut microbiomes in wild animals. *Microbiome Science and Medicine*, *1*(1). https://doi.org/10.2478/micsm-2013-0002

Amir, A., McDonald, D., Navas-Molina, J. A., Kopylova, E., Morton, J. T., Zech Xu, Z., Kightley, E. P., Thompson, L. R., Hyde, E. R., Gonzalez, A., & Knight, R. (2017). Deblur Rapidly Resolves Single-Nucleotide Community Sequence Patterns. *mSystems*, *2*(2), e00191-16. https://doi.org/10.1128/mSystems.00191-16

Anderson, M. J. (2017). Permutational Multivariate Analysis of Variance (PERMANOVA). In *Wiley StatsRef: Statistics Reference Online* (pp. 1–15). John Wiley & Sons, Ltd. https://doi.org/10.1002/9781118445112.stat07841

Anderson, M. J., & Braak, C. T. (2003). Permutation tests for multi-factorial analysis of variance. *Journal of Statistical Computation and Simulation*, *73*(2), 85–113. https://doi.org/10.1080/00949650215733

Andrews, S. (2010). *Babraham Bioinformatics—FastQC A Quality Control tool for High Throughput Sequence Data* [Computer software]. https://www.bioinformatics.babraham.ac.uk/projects/fastqc/

Arnold, P. A., Delean, S., Cassey, P., & White, C. R. (2021). Meta-analysis reveals that resting metabolic rate is not consistently related to fitness and performance in animals. *Journal of Comparative Physiology B*, *191*(6), 1097–1110. https://doi.org/10.1007/s00360-021-01358-w

Auer, S. K., Dick, C. A., Metcalfe, N. B., & Reznick, D. N. (2018). Metabolic rate evolves rapidly and in parallel with the pace of life history. *Nature Communications*, *9*, 14. https://doi.org/10.1038/s41467-017-02514-z

Auer, S. K., Salin, K., Rudolf, A. M., Anderson, G. J., & Metcalfe, N. B. (2015). Flexibility in metabolic rate confers a growth advantage under changing food availability. *Journal of Animal Ecology*, *84*(5), 1405–1411. https://doi.org/10.1111/1365-2656.12384

Bartoń, K. (2026). *MuMIn: Multi-model inference* [Manual]. https://doi.org/10.32614/CRAN.package.MuMIn

Bates, D., Mächler, M., Bolker, B., & Walker, S. (2015). Fitting Linear Mixed-Effects Models Using **lme4**. *Journal of Statistical Software*, *67*(1). https://doi.org/10.18637/jss.v067.i01

Bergman, E. N. (1990). Energy contributions of volatile fatty acids from the gastrointestinal tract in various species. *Physiological Reviews*, *70*(2), 567–590. https://doi.org/10.1152/physrev.1990.70.2.567

Bisanz, J. E. (2018). *qiime2R: Importing QIIME2 artifacts and associated data into R sessions*. https://github.com/jbisanz/qiime2R

Bokulich, N. A., Kaehler, B. D., Rideout, J. R., Dillon, M., Bolyen, E., Knight, R., Huttley, G. A., & Gregory Caporaso, J. (2018). Optimizing taxonomic classification of marker-gene amplicon sequences with QIIME 2's q2-feature-classifier plugin. *Microbiome*, *6*(1), 90. https://doi.org/10.1186/s40168-018-0470-z

Bokulich, N. A., Subramanian, S., Faith, J. J., Gevers, D., Gordon, J. I., Knight, R., Mills, D. A., & Caporaso, J. G. (2013). Quality-filtering vastly improves diversity estimates from Illumina amplicon sequencing. *Nature Methods*, *10*(1), 57–59. https://doi.org/10.1038/nmeth.2276

Bolyen, E., Rideout, J. R., Dillon, M. R., Bokulich, N. A., Abnet, C. C., Al-Ghalith, G. A., Alexander, H., Alm, E. J., Arumugam, M., Asnicar, F., Bai, Y., Bisanz, J. E., Bittinger, K., Brejnrod, A., Brislawn, C. J., Brown, C. T., Callahan, B. J., Caraballo-Rodríguez, A. M., Chase, J., … Caporaso, J. G. (2019). Reproducible, interactive, scalable and extensible microbiome data science using QIIME 2. *Nature Biotechnology*, *37*(8), 852–857. https://doi.org/10.1038/s41587-019-0209-9

Bordenstein, S. R., & Theis, K. R. (2015). Host Biology in Light of the Microbiome: Ten Principles of Holobionts and Hologenomes. *PLOS Biology*, *13*(8), e1002226. https://doi.org/10.1371/journal.pbio.1002226

Bourdeau-Julien, I., Castonguay-Paradis, S., Rochefort, G., Perron, J., Lamarche, B., Flamand, N., Di Marzo, V., Veilleux, A., & Raymond, F. (2023). The diet rapidly and differentially affects the gut microbiota and host lipid mediators in a healthy population. *Microbiome*, *11*(1), 26. https://doi.org/10.1186/s40168-023-01469-2

Burton, T., Killen, S. S., Armstrong, J. D., & Metcalfe, N. B. (2011). What causes intraspecific variation in resting metabolic rate and what are its ecological

consequences? *Proceedings of the Royal Society B: Biological Sciences*, *278*(1724), 3465–3473. https://doi.org/10.1098/rspb.2011.1778

Chuvochina, M., Gerken, J., Frentrup, M., Sandikci, Y., Goldmann, R., Freese, H. M., Göker, M., Sikorski, J., Yarza, P., Quast, C., Peplies, J., Glöckner, F. O., & Reimer, L. C. (2026). SILVA in 2026: A global core biodata resource for rRNA within the DSMZ digital diversity. *Nucleic Acids Research*, *54*(D1), D334–D341. https://doi.org/10.1093/nar/gkaf1247

Dapa, T., Wong, D. P., Vasquez, K. S., Xavier, K. B., Huang, K. C., & Good, B. H. (2023). Within-host evolution of the gut microbiome. *Current Opinion in Microbiology*, *71*, 102258. https://doi.org/10.1016/j.mib.2022.102258

David, L. A., Maurice, C. F., Carmody, R. N., Gootenberg, D. B., Button, J. E., Wolfe, B. E., Ling, A. V., Devlin, A. S., Varma, Y., Fischbach, M. A., Biddinger, S. B., Dutton, R. J., & Turnbaugh, P. J. (2014). Diet rapidly and reproducibly alters the human gut microbiome. *Nature*, *505*(7484), 559–563. https://doi.org/10.1038/nature12820

Davis, N. M., Proctor, D., Holmes, S. P., Relman, D. A., & Callahan, B. J. (2017). Simple statistical identification and removal of contaminant sequences in marker-gene and metagenomics data. *bioRxiv : The Preprint Server for Biology*, 221499. https://doi.org/10.1101/221499

den Besten, G., van Eunen, K., Groen, A. K., Venema, K., Reijngoud, D.-J., & Bakker, B. M. (2013). The role of short-chain fatty acids in the interplay between diet, gut microbiota, and host energy metabolism. *Journal of Lipid Research*, *54*(9), 2325–2340. https://doi.org/10.1194/jlr.R036012

Desai, M., & Hales, C. N. (1997). Role of Fetal and Infant Growth in Programming Metabolism in Later Life. *Biological Reviews*, *72*(2), 329–348. https://doi.org/10.1111/j.1469-185X.1997.tb00016.x

Donohoe, D. R., Garge, N., Zhang, X., Sun, W., O'Connell, T. M., Bunger, M. K., & Bultman, S. J. (2011). The Microbiome and Butyrate Regulate Energy Metabolism and Autophagy in the Mammalian Colon. *Cell Metabolism*, *13*(5), 517–526. https://doi.org/10.1016/j.cmet.2011.02.018

Doolittle, W. F., & Booth, A. (2017). It's the song, not the singer: An exploration of holobiosis and evolutionary theory. *Biology & Philosophy*, *32*(1), 5–24. https://doi.org/10.1007/s10539-016-9542-2

Ewels, P., Magnusson, M., Lundin, S., & Käller, M. (2016). MultiQC: Summarize analysis results for multiple tools and samples in a single report. *Bioinformatics*, *32*(19), 3047–3048. https://doi.org/10.1093/bioinformatics/btw354

Fusco, W., Lorenzo, M. B., Cintoni, M., Porcari, S., Rinninella, E., Kaitsas, F., Lener, E., Mele, M. C., Gasbarrini, A., Collado, M. C., Cammarota, G., & Ianiro, G. (2023). Short-Chain Fatty-Acid-Producing Bacteria: Key Components of the Human Gut Microbiota. *Nutrients*, *15*(9), 2211. https://doi.org/10.3390/nu15092211

Gilley, S. P., Ruebel, M. L., Chintapalli, S. V., Wright, C. J., Rozance, P. J., & Shankar, K. (2024). Calorie restriction during gestation impacts maternal and offspring fecal microbiome in mice. *Frontiers in Endocrinology*, *15*, 1423464. https://doi.org/10.3389/fendo.2024.1423464

Gutiérrez, N., & Garrido, D. (2019). Species Deletions from Microbiome Consortia Reveal Key Metabolic Interactions between Gut Microbes. *mSystems*, *4*(4), 10.1128/msystems.00185-19. https://doi.org/10.1128/msystems.00185-19

Hanhimäki, E., Watts, P. C., Koskela, E., Koteja, P., Mappes, T., & Hämäläinen, A. M. (2022). Evolved high aerobic capacity has context-specific effects on gut microbiota. *Frontiers in Ecology and Evolution*, *10*, 934164. https://doi.org/10.3389/fevo.2022.934164

Hartig, F. (2024). *DHARMa: Residual diagnostics for hierarchical (multi-level / mixed) regression models* [Manual]. https://doi.org/10.32614/CRAN.package.DHARMa

Holscher, H. D. (2017). Dietary fiber and prebiotics and the gastrointestinal microbiota. *Gut Microbes*, *8*(2), 172–184. https://doi.org/10.1080/19490976.2017.1290756

Hseiky, A., Sadowska, E. T., & Koteja, P. (2026). The effects of short-term consumption of a Western diet on aerobic exercise performance in bank voles with inherently distinct metabolic rates. *Experimental Physiology*, *111*(3), 930–945. https://doi.org/10.1113/EP092646

Jaromin, E., Sadowska, E. T., & Koteja, P. (2019). Is Experimental Evolution of an Increased Aerobic Exercise Performance in Bank Voles Mediated by Endocannabinoid Signaling Pathway? *Frontiers in Physiology*, *10*. https://doi.org/10.3389/fphys.2019.00640

Kim, S., Park, S., Ansari, A., Lee, G., Hur, Y. M., An, J., Lee, S. S., You, Y., & Kim, Y. J. (2025). Altered Abundance of Butyrate-Producing Lachnospiraceae by Maternal

Diet During Pregnancy Potentially Influences MASLD-Related Lipid Dysregulation in Male Rat Offspring. *Molecular Nutrition & Food Research*, *69*(19), e70153. https://doi.org/10.1002/mnfr.70153

Kuznetsova, A., Brockhoff, P. B., & Christensen, R. H. B. (2017). **lmerTest** Package: Tests in Linear Mixed Effects Models. *Journal of Statistical Software*, *82*(13). https://doi.org/10.18637/jss.v082.i13

Lamichhane, S., Salihovic, S., Sinioja, T., Virtanen, S. M., Vatanen, T., Orešič, M., Knip, M., & Hyötyläinen, T. (2026). Prenatal exposure to persistent organic pollutants modulates the metabolism and gut microbiota of the offspring. *Environment International*, *208*, 110080. https://doi.org/10.1016/j.envint.2026.110080

Lenth, R. V., & Piaskowski, J. (2017). *emmeans: Estimated Marginal Means, aka Least-Squares Means* (p. 2.0.3). https://doi.org/10.32614/CRAN.package.emmeans

Lin, H. (2026, April 27). *FrederickHuangLin/ANCOMBC*. https://github.com/FrederickHuangLin/ANCOMBC

Lin, H., Eggesbo, M., & Peddada, S. D. (2022). Linear and nonlinear correlation estimators unveil undescribed taxa interactions in microbiome data. *Nature Communications*, *13*(1), 1–16.

Lin, H., & Peddada, S. D. (2020). Analysis of compositions of microbiomes with bias correction. *Nature Communications*, *11*(1), 1–11.

Lin, H., & Peddada, S. D. (2024). Multigroup analysis of compositions of microbiomes with covariate adjustments and repeated measures. *Nature Methods*, *21*(1), 83–91.

Lipowska, M. M., Sadowska, E. T., Kohl, K. D., & Koteja, P. (2025). Experimental evolution of a mammalian holobiont: Bank voles selected for herbivorous capability evolved distinct and robust gut bacterial communities. *ISME Communications*, *5*(1), ycaf160. https://doi.org/10.1093/ismeco/ycaf160

Lipowska, M. M., Sadowska, E. T., Palme, R., & Koteja, P. (2022). Evolution of an increased performance under acute challenge does not exacerbate vulnerability to chronic stress. *Scientific Reports*, *12*(1), 2126. https://doi.org/10.1038/s41598-022-06060-7

Liu, X., Jin, Z., Summers, S., Derous, D., Li, M., Li, B., Li, L., & Speakman, J. R. (2022). Calorie restriction and calorie dilution have different impacts on body fat,

metabolism, behavior, and hypothalamic gene expression. *Cell Reports*, *39*(7), 110835. https://doi.org/10.1016/j.celrep.2022.110835

Lundgren, S. N., Madan, J. C., Emond, J. A., Morrison, H. G., Christensen, B. C., Karagas, M. R., & Hoen, A. G. (2018). Maternal diet during pregnancy is related with the infant stool microbiome in a delivery mode-dependent manner. *Microbiome*, *6*, 109. https://doi.org/10.1186/s40168-018-0490-8

Martínez-Oca, P., Alba, C., Sánchez-Roncero, A., Fernández-Marcelo, T., Martín, M. Á., Escrivá, F., Rodríguez, J. M., Álvarez, C., & Fernández-Millán, E. (2023). Maternal Diet Determines Milk Microbiome Composition and Offspring Gut Colonization in Wistar Rats. *Nutrients*, *15*(20), 4322. https://doi.org/10.3390/nu15204322

Martino, C., Dilmore, A. H., Burcham, Z. M., Metcalf, J. L., Jeste, D., & Knight, R. (2022). Microbiota succession throughout life from the cradle to the grave. *Nature Reviews Microbiology*, *20*(12), 707–720. https://doi.org/10.1038/s41579-022-00768-z

Mayorga-Ramos, A., Barba-Ostria, C., Simancas-Racines, D., & Guamán, L. P. (2022). Protective role of butyrate in obesity and diabetes: New insights. *Frontiers in Nutrition*, *9*, 1067647. https://doi.org/10.3389/fnut.2022.1067647

McDonald, D., Clemente, J. C., Kuczynski, J., Rideout, J. R., Stombaugh, J., Wendel, D., Wilke, A., Huse, S., Hufnagle, J., Meyer, F., Knight, R., & Caporaso, J. G. (2012). The Biological Observation Matrix (BIOM) format or: How I learned to stop worrying and love the ome-ome. *GigaScience*, *1*(1), 7. https://doi.org/10.1186/2047-217X-1-7

McGillycuddy, M., Warton, D. I., Popovic, G., & Bolker, B. M. (2025). Parsimoniously Fitting Large Multivariate Random Effects in **glmmTMB**. *Journal of Statistical Software*, *112*(1). https://doi.org/10.18637/jss.v112.i01

McKinney, W. (2010). *Data Structures for Statistical Computing in Python*. 56–61. https://doi.org/10.25080/Majora-92bf1922-00a

McMurdie, P. J., & Holmes, S. (2013). phyloseq: An R package for reproducible interactive analysis and graphics of microbiome census data. *PLoS ONE*, *8*(4), e61217.

McMurdie, P. J., & Holmes, S. (2014). Waste Not, Want Not: Why Rarefying Microbiome Data Is Inadmissible. *PLOS Computational Biology*, *10*(4), e1003531. https://doi.org/10.1371/journal.pcbi.1003531

Milani, C., Duranti, S., Bottacini, F., Casey, E., Turroni, F., Mahony, J., Belzer, C., Delgado Palacio, S., Arboleya Montes, S., Mancabelli, L., Lugli, G. A., Rodriguez, J. M., Bode, L., de Vos, W., Gueimonde, M., Margolles, A., van Sinderen, D., & Ventura, M. (2017). The First Microbial Colonizers of the Human Gut: Composition, Activities, and Health Implications of the Infant Gut Microbiota. *Microbiology and Molecular Biology Reviews*, *81*(4), 10–1128. https://doi.org/10.1128/mmbr.00036-17

Morrison, D. J., & Preston, T. (2016). Formation of short chain fatty acids by the gut microbiota and their impact on human metabolism. *Gut Microbes*, *7*(3), 189–200. https://doi.org/10.1080/19490976.2015.1134082

Oksanen, J., Simpson, G. L., Blanchet, F. G., Kindt, R., Legendre, P., Minchin, P. R., O'Hara, R. B., Solymos, P., Stevens, M. H. H., Szoecs, E., Wagner, H., Barbour, M., Bedward, M., Bolker, B., Borcard, D., Borman, T., Carvalho, G., Chirico, M., De Caceres, M., … Weedon, J. (2026). *vegan: Community ecology package* [Manual]. https://CRAN.R-project.org/package=vegan

Oksanen, T. A., Jonsson, P., Koskela, E., & Mappes, T. (2001). Optimal allocation of reproductive effort: Manipulation of offspring number and size in the bank vole. *Proceedings of the Royal Society of London. Series B: Biological Sciences*, *268*(1467), 661–666. https://doi.org/10.1098/rspb.2000.1409

Palou, M., Priego, T., Sánchez, J., Torrens, J. M., Palou, A., & Picó, C. (2010). Moderate Caloric Restriction in Lactating Rats Protects Offspring against Obesity and Insulin Resistance in Later Life. *Endocrinology*, *151*(3), 1030–1041. https://doi.org/10.1210/en.2009-0934

Pedregosa, F., Varoquaux, G., Gramfort, A., Michel, V., Thirion, B., Grisel, O., Blondel, M., Prettenhofer, P., Weiss, R., Dubourg, V., Vanderplas, J., Passos, A., Cournapeau, D., Brucher, M., Perrot, M., & Duchesnay, É. (2011). Scikit-learn: Machine Learning in Python. *The Journal of Machine Learning Research*, *12*, 2825–2830.

Processing, filtering, and evaluating the SILVA database (and other reference sequence data) with RESCRIPt—Community Contributions / Tutorials. (2020, June 25). QIIME 2 Forum. https://forum.qiime2.org/t/processing-filtering-and-evaluating-the-silva-database-and-other-reference-sequence-data-with-rescript/15494

R Core Team. (2025). *R: a language and environment for statistical computing* [Manual]. R Foundation for Statistical Computing. https://www.R-project.org/

Robeson, M. S., O'Rourke, D. R., Kaehler, B. D., Ziemski, M., Dillon, M. R., Foster, J. T., & Bokulich, N. A. (2021). RESCRIPt: Reproducible sequence taxonomy reference database management. *PLOS Computational Biology*, *17*(11), e1009581. https://doi.org/10.1371/journal.pcbi.1009581

Rosenberg, E., & Zilber-Rosenberg, I. (2018). The hologenome concept of evolution after 10 years. *Microbiome*, *6*(1), 1–14. https://doi.org/10.1186/s40168-018-0457-9

Sadowska, E. T., Baliga-Klimczyk, K., Chrząścik, K. M., & Koteja, P. (2008). Laboratory Model of Adaptive Radiation: A Selection Experiment in the Bank Vole. *Physiological and Biochemical Zoology*, *81*(5), 627–640. https://doi.org/10.1086/590164

Sadowska, E. T., Labocha, M. K., Baliga, K., Stanisz, A., Wróblewska, A. K., Jagusiak, W., & Koteja, P. (2005). Genetic correlations between basal and maximum metabolic rates in a wild rodent: Consequences for evolution of endothermy. *Evolution*, *59*(3), 672–681. https://doi.org/10.1111/j.0014-3820.2005.tb01025.x

Schloss, P. D. (2024). Rarefaction is currently the best approach to control for uneven sequencing effort in amplicon sequence analyses. *mSphere*, *9*(2), e0035423. https://doi.org/10.1128/msphere.00354-23

Speakman, J. R., & Król, E. (2005). Limits to sustained energy intake IX: A review of hypotheses. *Journal of Comparative Physiology B*, *175*(6), 375–394. https://doi.org/10.1007/s00360-005-0013-3

Stewart, C. J., Ajami, N. J., O'Brien, J. L., Hutchinson, D. S., Smith, D. P., Wong, M. C., Ross, M. C., Lloyd, R. E., Doddapaneni, H., Metcalf, G. A., Muzny, D., Gibbs, R. A., Vatanen, T., Huttenhower, C., Xavier, R. J., Rewers, M., Hagopian, W., Toppari, J., Ziegler, A.-G., … Petrosino, J. F. (2018). Temporal development of the gut microbiome in early childhood from the TEDDY study. *Nature*, *562*(7728), 583–588. https://doi.org/10.1038/s41586-018-0617-x

Turnbaugh, P. J., Ley, R. E., Mahowald, M. A., Magrini, V., Mardis, E. R., & Gordon, J. I. (2006). An obesity-associated gut microbiome with increased capacity for energy harvest. *Nature*, *444*(7122), 1027–1031. https://doi.org/10.1038/nature05414

Vacca, M., Celano, G., Calabrese, F. M., Portincasa, P., Gobbetti, M., & De Angelis, M. (2020). The Controversial Role of Human Gut Lachnospiraceae. *Microorganisms*, *8*(4), 573. https://doi.org/10.3390/microorganisms8040573

Voolstra, C. R., & Ziegler, M. (2020). Adapting with Microbial Help: Microbiome Flexibility Facilitates Rapid Responses to Environmental Change. *BioEssays*, *42*(7), 2000004. https://doi.org/10.1002/bies.202000004

Walters, A. W., Hughes, R. C., Call, T. B., Walker, C. J., Wilcox, H., Petersen, S. C., Rudman, S. M., Newell, P. D., Douglas, A. E., Schmidt, P. S., & Chaston, J. M. (2020). The microbiota influences the Drosophila melanogaster life history strategy. *Molecular Ecology*, *29*(3), 639–653. https://doi.org/10.1111/mec.15344

Waters, J. L., & Ley, R. E. (2019). The human gut bacteria Christensenellaceae are widespread, heritable, and associated with health. *BMC Biology*, *17*, 83. https://doi.org/10.1186/s12915-019-0699-4

Wei, Y., Gao, J., Kou, Y., Meng, L., Zheng, X., Liang, M., Sun, H., Liu, Z., & Wang, Y. (2020). Commensal Bacteria Impact a Protozoan's Integration into the Murine Gut Microbiota in a Dietary Nutrient-Dependent Manner. *Applied and Environmental Microbiology*, *86*(11), e00303-20. https://doi.org/10.1128/AEM.00303-20

Wen, S., Yuan, G., Li, C., Xiong, Y., Zhong, X., & Li, X. (2022). High cellulose dietary intake relieves asthma inflammation through the intestinal microbiome in a mouse model. *PLOS ONE*, *17*(3), e0263762. https://doi.org/10.1371/journal.pone.0263762

Wickham, H. (2016). *ggplot2: Elegant graphics for data analysis*. Springer-Verlag New York. https://ggplot2.tidyverse.org

Wilke, C. O. (2025). *cowplot: Streamlined plot theme and plot annotations for "ggplot2"* [Manual]. https://doi.org/10.32614/CRAN.package.cowplot